

Review

Porous Aerogel Structures as Promising Materials for Photocatalysis, Thermal Insulation Textiles, and Technical Applications: A Review

Kang Hoon Lee ¹, Zafar Arshad ^{2,*}, Alla Dahshan ³, Mubark Alshareef ⁴, Qana A. Alsulami ^{5,*}, Ayesha Bibi ⁶, Eui-Jong Lee ⁷, Muddasir Nawaz ⁸, Usman Zubair ² and Amjed Javid ²

- ¹ Department of Energy and Environmental Engineering, The Catholic University of Korea, 43 Jibong-ro, Bucheon-si 14662, Republic of Korea; diasyoung@catholic.ac.kr
 - ² School of Engineering and Technology, National Textile University Faisalabad, Faisalabad 37610, Pakistan; usmank980@gmail.com (U.Z.); amjedljno907@gmail.com (A.J.)
 - ³ Department of Physics, Faculty of Science, King Khalid University, P.O. Box 9004, Abha 62529, Saudi Arabia; adahshan73@gmail.com
 - ⁴ Department of Chemistry, Faculty of Applied Science, Umm Al Qura University, Makkah 24230, Saudi Arabia; mmshreef@uqu.edu.sa
 - ⁵ Chemistry Department, Faculty of Science, King Abdulaziz University, Jeddah 21589, Saudi Arabia
 - ⁶ Department of Human Nutrition and Dietetics, Women University Mardan, Mardan 23200, Pakistan; ayeshabb2009@yahoo.com
 - ⁷ Department of Environmental Engineering, Daegu University, 201 Daegudae-ro, Jillyang, Gyeongsan-si 38453, Republic of Korea; lujong@daegu.ac.kr
 - ⁸ Centre for Advance Materials, Qatar University, Doha P.O. Box 2713, Qatar; m.nawaz@qu.edu.qa
- * Correspondence: zafarnubii@gmail.com (Z.A.); qalselami@kau.edu.sa (Q.A.A.)



Citation: Lee, K.H.; Arshad, Z.; Dahshan, A.; Alshareef, M.; Alsulami, Q.A.; Bibi, A.; Lee, E.-J.; Nawaz, M.; Zubair, U.; Javid, A. Porous Aerogel Structures as Promising Materials for Photocatalysis, Thermal Insulation Textiles, and Technical Applications: A Review. *Catalysts* **2023**, *13*, 1286. <https://doi.org/10.3390/catal13091286>

Academic Editor: Narendra Kumar

Received: 19 June 2023

Revised: 29 August 2023

Accepted: 3 September 2023

Published: 8 September 2023

Corrected: 7 December 2023



Copyright: © 2023 by the authors. Licensee MDPI, Basel, Switzerland. This article is an open access article distributed under the terms and conditions of the Creative Commons Attribution (CC BY) license (<https://creativecommons.org/licenses/by/4.0/>).

Abstract: Aerogels, due to their unique features like lightweight, ultra-low thermal conductivity, and design variations, have gotten a lot of interest in thermal insulation, photocatalysis, and protective areas. Besides their superior thermal properties, aerogel thermal insulation and photocatalyst materials also possess many inherent flaws, such as handling issues, high manufacturing costs, and low strength as well as toughness. The most persuasive and successful ways to improve photocatalytic and thermal insulating qualities while lowering costs are composition optimization and microstructure reconstruction. Their high surface area and porosity make them ideal for enhancing the efficiency and capacity of these devices. Research may lead to more efficient and longer-lasting energy storage solutions. This review describes the characteristics, microstructural reconstruction, design variation, and properties of all aerogel fabrication techniques and provides a comprehensive overview of scientific achievements linked to them. The effectiveness of raw material compositions, properties, and mechanical parameters are also discussed. The major goal of this review is to highlight the aerogel-based materials and design variations and to explore the most potential development trends for photocatalysis and thermal applications. The industrial as well as technical applications of silica aerogels are also highlighted. This review highlights futuristic applications of aerogel-based textile materials to alleviate the CO₂ burden on our atmosphere, either by providing next-level thermal insulation or by employing them in CO₂ mitigating technologies such as CO₂ capture.

Keywords: thermal insulation; photocatalysis; specific heat; aerogel porosity; mesoporous layer; thermal conductivity

1. General Aerogel Overview

Aerogels have been discovered as the most promising thermally insulated material for textile, industrial, and other protective applications. These materials, having the highest porosity, are also highly recommended for thermal insulation, purification, energy storage, and catalysis [1,2]. It emphasizes the recent contribution of aerogels with their surface

modification, material variation, and fascinating optical characteristics [3,4]. The global energy crisis and environmental degradation are getting increasingly critical as national economies develop rapidly [5]. Energy demand has increased at a rate of 1.8% per year over the past 40 years, rising from 2790 Mtoe in 2010 to nearly 4400 Mtoe by 2050 [6]. Energy conservation utilizes all natural resources—gas, oil, coal, and nuclear energy—as a potential resource for energy conservation. During the era of 2016–2020, China was very much intended to meet its domestic economic lines by all possible means. China invested almost 1.2 trillion RMB in its energy conservation sector and environmental protection [7]. The European Union also anticipated that all energy-efficient buildings toward green conservation by the end of 2020 [8]. United Union planned to maintain all commercial buildings with energy-efficient infrastructure to meet the current energy demands of the sector. The introduction of new and innovative thermal insulation materials has been of greater interest to researchers involved in maintaining environmental structures and thermal equipment [9,10].

Conventional thermal insulation materials and fabrications demand high-cost raw materials, multiple fabrication layers, and high costs [11]. As aerogels are lightweight and highly thermal insulators, they have the capability to replace conventional ones with superior insulating characteristics [12]. Aerogels have shown tremendous potential for various applications due to their unique properties. These ultralight materials are known for their extremely low density, high surface area, and excellent thermal insulating properties, as shown in Figure 1 [13,14]. Aerogels' porosity varies in the nanometer-scale range, with pores of 1/3000th the diameter [3,12]. It has a series of networks with an air volume of around 80–99.8% and a surface area of 100–1600 m²g⁻¹. Due to the low refractive index value (1.007–1.240), these materials are highly preferred for insulation purposes, laser experiments, nuclear particle detection, and ultrasonic gas sensors. It can behave like a superheat insulator in thermal applications [15]. Aerogels have a unique and intricate structure that contributes to their exceptional properties. They are often referred to as “frozen smoke” due to their translucent appearance and extremely low density. There are three basic parts: two solid parts and one porous part. The porous part is sandwiched, preserving the aerogel's structure [16,17]. In aerogels, the liquid is replaced by air with shrinkage of the solid network, achieving the highest porosity. When the liquid component of gel is replaced with air, higher porosity provides superior results. Its porosity lies at both meso and micro levels [18].

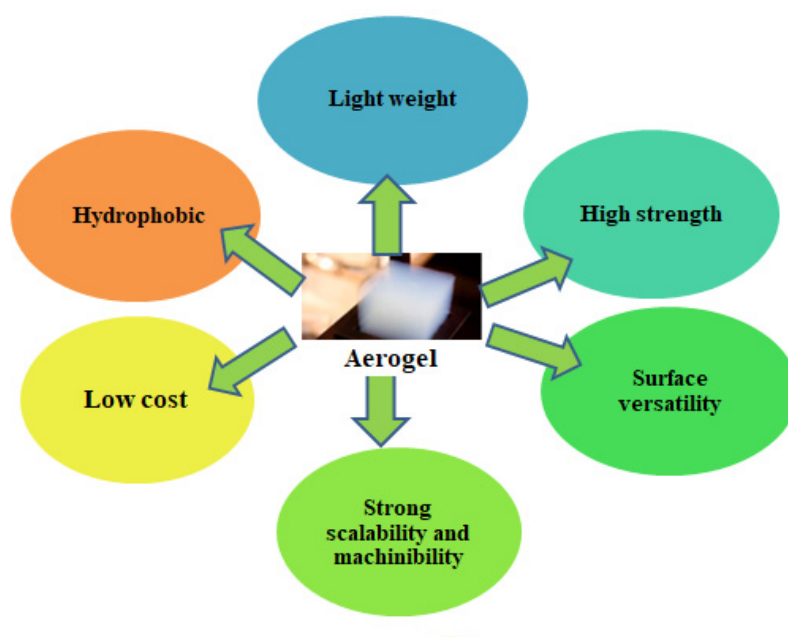


Figure 1. Aerogel characteristics.

2. History and Marketing

Aerogel was first discovered by Samuel Stephens Kistler in 1931. It was also named solid smoke, blue air, or frozen smoke. In the 1990s, it was a promising candidate for thermal insulation, flameproofing, and other lighter-weight applications. In the 21st century, aerogel materials were a potential research area [19]. Around 2013–2020, aerogel marketing jumped up to US\$ 1896.6 million from \$221.8 million, and now it is expected to boom up to \$1395 million by 2027. The growth of aerogel marketing is mainly due to the increased development of the build-tech and geo-tech sectors [20]. The top leading manufacturers of aerogel are Aerogel Technologies Leading Large Crystallographic Aerogels (LLCA), Armacell International Silica Aerogels (SA), Thermablok Aerogels Limited, JIOS Aerogel, Cabot Corporation, and Aspen Aerogel Corporation [21].

Factors Affecting the Aerogel Market

There are some limiting factors due to which the aerogel market is badly affected. Mainly, these factors are the expensive processing parameters of aerogel synthesis and higher production costs. Aerogel synthesis requires higher cost rates of raw materials to produce a market-competent product, thereby negatively impacting the market growth [22]. Scientists are highly focused on reducing production costs and making more customer-attractive products for aerogel marketing. Increasing product applications in multiple areas is an attractive way to improve marketing [23].

Public awareness about the advanced applications of aerogel-based materials in the field of insulation and other purposes can increase the market growth rate. The aerogel market is influenced by a combination of technological, economic, and societal factors. These factors can impact the demand, production, and adoption of aerogels in various industries [24,25]. The marketing and applications of aerogels are also categorized as exotic areas because of their peculiar characteristics and natural accessibility [26]. Silica is the most versatile aerogel material being used worldwide for thermal isolation, as shown in Figure 2.

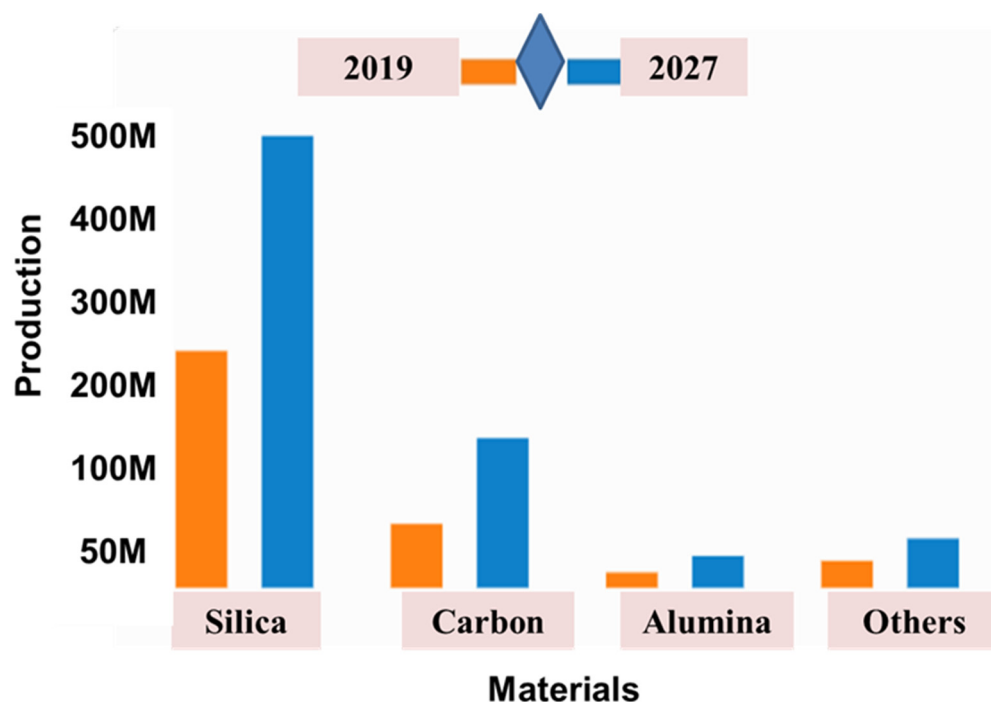


Figure 2. Growth rate market of different aerogel-based materials [14].

3. Aerogel Chemistry

Aerogel is a nanoporous polymeric material (Figure 3) with a backbone of linked nanoparticles (15 nm) that expand throughout its volume due to gas expansion, forming a 3D continuous network. Aerogel materials are 15 times heavier as compared to air, which has a very low dielectric constant [27]. Aerogel materials possess higher sound absorption but a low sound velocity [28] with damping > 50 dB and air velocity around ≈ 100 m/s. Aerogel possesses a very low thermal conductivity of 0.005–0.1 W/m·K. Aerogel's physical structure can be transparent or opaque, or it can be colored and have a variable refractive index (1001 to 2.1) [29]. Aerogel materials have internal surface areas ranging from 10–2000 m²/g. Aerogel surfaces can be functionalized and made hydrophobic by polymeric residues with the help of chemical vapor deposition (CVD) of magnetic layers. Gel structure is basically functionalized by embedded particles (e.g., dyes, ferroelectrics) or with interpenetrating hybrid aerogel networks [21,30,31].

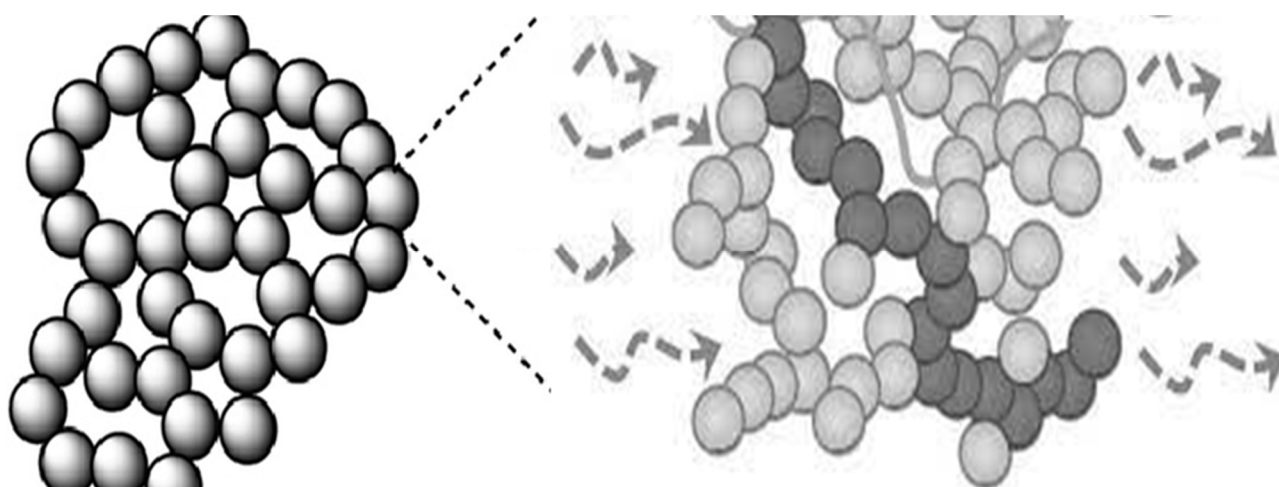


Figure 3. Aerogel structure. Reproduced from [32].

4. Aerogel Porosity and Calculations

Per International Union of Pure and Applied Chemistry (IUPAC) standards, pore size < 2 nm is termed as microporous, pore size 2–50 nm is termed as mesoporous, and pores > 50 nm are macroporous. Synthesized aerogels are varied from microporous to mesoporous structure; however, most of them are mesoporous, as shown in Figure 4. In aerogel pore networking, the pore size should be in that range where liquid can easily flow from pore to pore. The liquid should be able to flow through the whole structure without any restriction. Aerogels are unique materials with the highest porosity and smaller pore size diameters [18,33]. For the calculation of the pore size, the BET/nitrogen adsorption method is utilized. In this technique, adsorbed gas is measured to detect pore size. Ball milling was used to reduce the particle size [34]. Figure 4a presents the comparison of aerogels loaded with silica and titania through BET analysis. The presence of silica concentration affects the pore size of aerogels, thereby enhancing the mechanical properties of aerogels as $P/P_0 = 0.99$, where P is the pressure of the substrate and P_0 is the inherent pressure. From the observation, titania-based aerogel surface area is 529–587 m²/g, whereas pore diameter ranges from 11.6 to 12.3 nm. For silica-based aerogels, the surface area equals 572.1 m²/g, whereas the pore diameter is 12.1 nm. According to IUPAC standards and desorption hysteresis, both of these are mesoporous aerogels. However, there is a significant difference in both densities, as carbon-based materials exhibited more density due to their inherent characteristics [35,36].

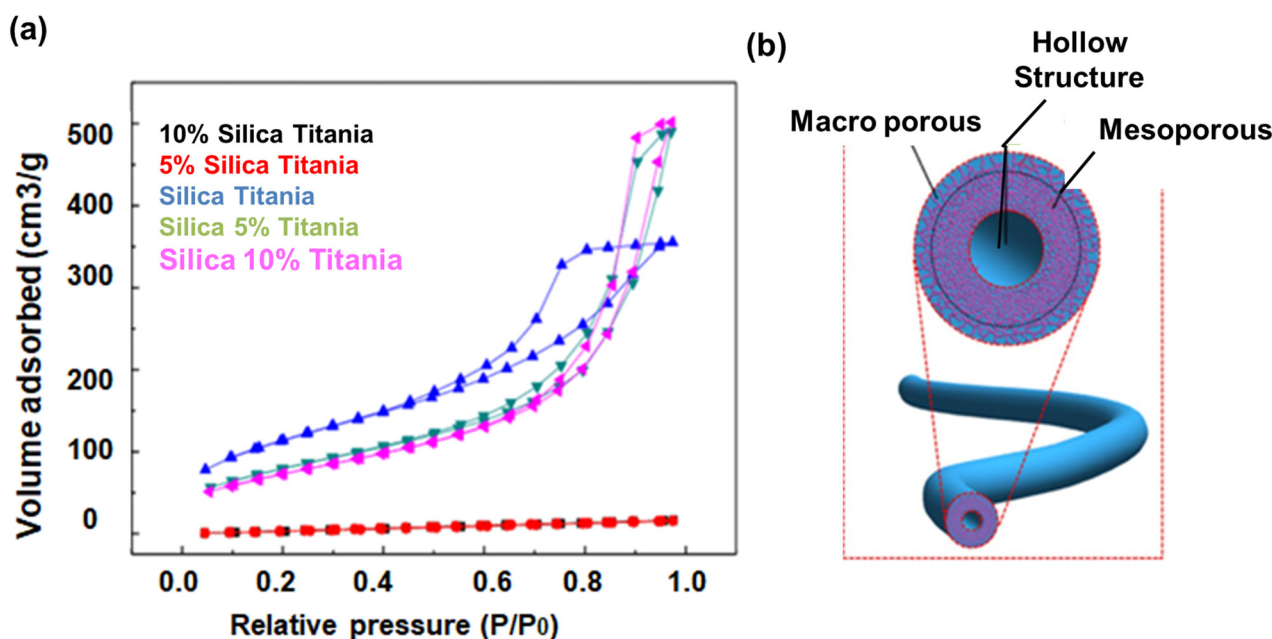


Figure 4. (a) BET Comparison between silica and titania-based aerogels; (b) Variations in aerogel as macrostructure and microstructures. Open access, reproduced from [37].

Volume shrinkage is calculated from the aerogel volume. There are two terms for understanding aerogel porosity: bulk density and skeletal density.

$$\text{Bulk density} = \frac{\text{Aerogel mass}}{\text{Aerogel volume}} \quad (1)$$

$$\text{Skeletal density} = \frac{\text{Mass of solid material}}{\text{Sum of the volume of solid material}} \quad (2)$$

Skeletal density value is almost closer to the bulk density. These two values are gained by the helium pycnometry [38].

Volume shrinkage percentage, porosity, and pore volume for aerogel are obtained by following formulae:

$$V_s(\% \text{age}) = \left(1 - \frac{V_a}{V_g}\right) \times 100 \quad (3)$$

$$\text{Porosity} = \left(1 - \frac{P_b}{P_s}\right) \times 100 \quad (4)$$

$$\text{Pore volume} = \left(\frac{1}{P_b} - \frac{1}{P_s}\right) \quad (5)$$

In the above equations, V_a is the volume of aerogels, V_g is the volume of air, P_b is the density of aerogels, whereas P_s is the density of base material, i.e., (cellulose).

5. Aerogels as Catalysis

Catalysts are essential components for the treatment of air and water pollutants on the way to a sustainable and clean environment. As active heterogeneous catalysts for a number of catalytic and photocatalytic environmental remediation processes, aerogels made from diverse molecular precursors are well known [39]. Because of this, aerogels have been viewed as a bridge bridging the nano and macroworlds, where the building blocks can both maintain their original features and develop new ones through their 3D interaction. Aerogels are particularly promising for photocatalytic applications due to their specific qualities [40]. Aerogels have an incredibly high surface area, which provides a large number of active sites for photocatalytic reactions to occur. This increased surface

area allows for more interactions between the catalyst and the reactants, enhancing the efficiency of the reaction. In addition, the development of novel aerogel materials like graphene has encouraged the search for more mechanically stable and versatile aerogel photocatalysts [41]. The use has expanded to include solar energy conversion in addition to conventional environmental cleanup [42]. Aerogels have been explored and applied in various catalytic processes due to their unique properties and larger surface area [43]. One notable example of aerogels used in catalysis is their application as catalyst supports for heterogeneous catalysis. Heterogeneous catalysis involves the use of a solid catalyst to accelerate a chemical reaction between gaseous or liquid reactants. This type of aerogel-supported catalyst can be used not only in hydrogenation reactions but also in a wide range of other catalytic processes such as oxidation, hydrogenolysis, and more. The versatility of aerogels as catalyst supports enables their application in various industries, including fine chemicals, pharmaceuticals, petrochemicals, and environmental remediation [44].

It is important to note that the specific conditions, metal catalyst, and reactants used in such catalytic processes will vary depending on the target reaction and the desired outcome. As research in the field of aerogel-based catalysis continues, we can expect to see more tailored and efficient catalyst systems developed for a variety of chemical transformations as shown in Figure 5 [45].

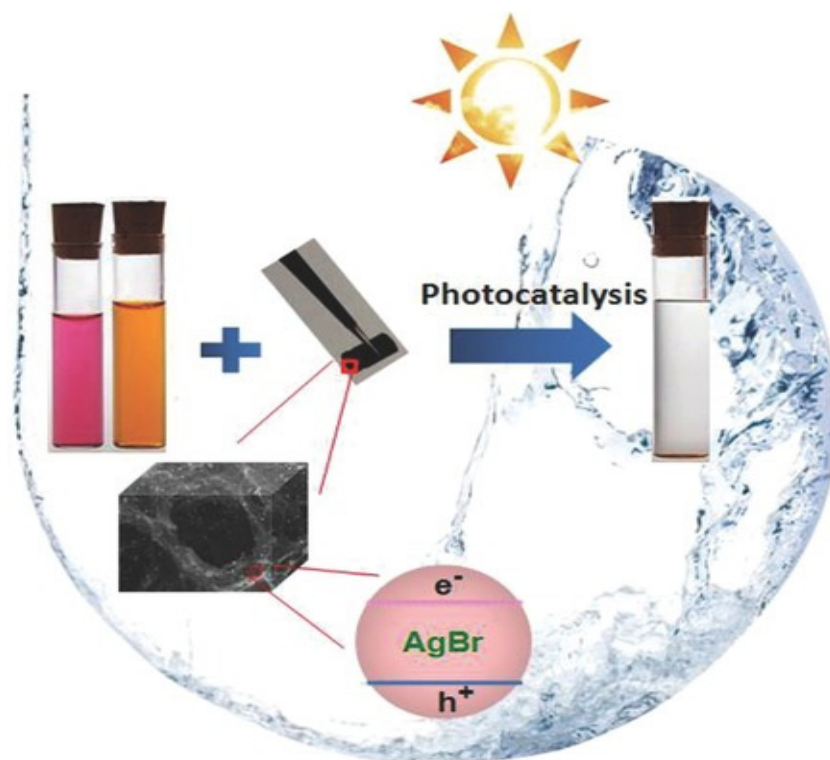


Figure 5. Aerogels as catalysis.

6. Aerogel Specific Heat

Specific heat is related to internal energy and is a very important thermodynamic property. The specific heat of aerogels is around 1900 J/g·K. Specific heat for volume and pressure is given in the following formulae:

$$Cv = \left(\frac{\partial u}{\partial T} \right) v \quad (6)$$

$$Cp = \left(\frac{\partial h}{\partial T} \right) p \quad (7)$$

In the above equations, u is internal energy, and h is enthalpy. T and P represent temperature and pressure [36]. Its SI units are $J/mol \cdot K$ or $J/Kg \cdot K$ [46]. In aerogel structures, free molecules are allowed to move randomly in the structure. On heating, the movement of free molecules increases and the volume of gas increases, thereby increasing the acceleration of aerogel-free molecules, as shown in Figure 6.

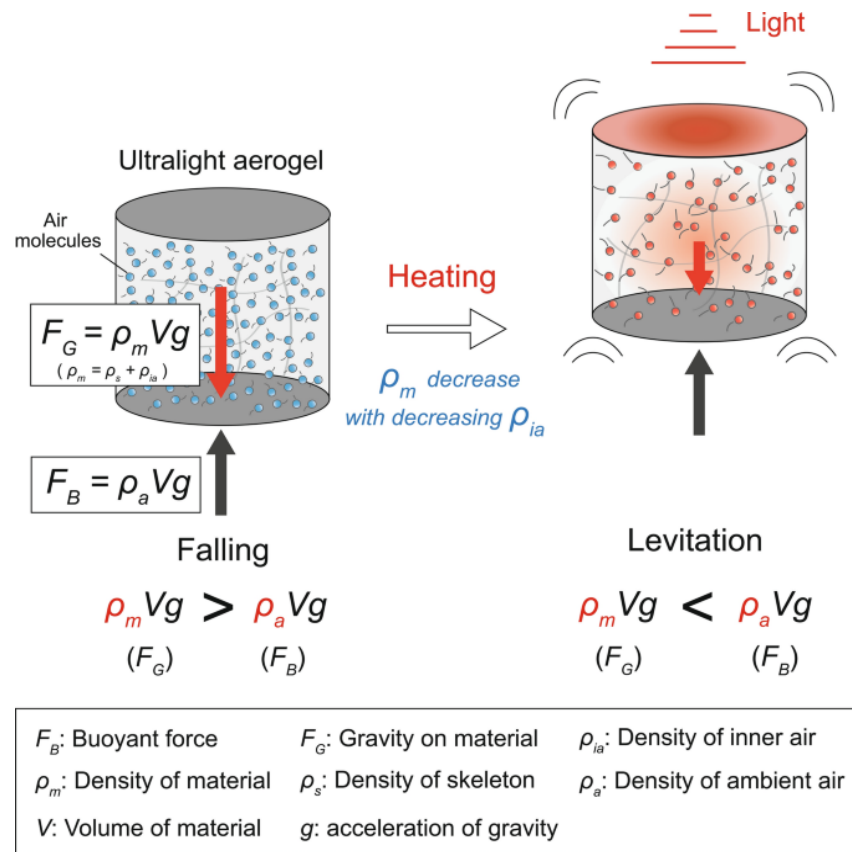


Figure 6. Aerogels specific heat measurements. Open access, Reproduced from [47].

7. Aerogel Heat Thermal Transfer Mechanism and Calculations

The heating transfer mechanism through hollow and aerogel fibers is termed “thermal conductivity”. It is measured in $W/m \cdot K$. It is measured with the basic principle of Fourier’s law, which is applicable to all fluids, gases, and liquids. Thermal conductivity varies with temperature, and it is termed as follows [48]:

$$k = k(\bar{r}, T(r, t)) = \frac{qx}{\partial T / \partial x} \tag{8}$$

As most of the materials are homogenous, $k = k(T)$.

As shown in Figure 7a, thermal conductivity via hollow fibers is as follows:

$$\lambda_1 = \lambda_{conv1} + \lambda_{cond1} + \lambda_{rad1} \tag{9}$$

In the above equation, λ_{conv} is basically the heat transfer through convection; λ_{cond} is basically the heat transfer via conduction; whereas λ_{rad} is the heat transfer through radiation. Hollow fibers possess a porosity of around 85%, so heat transfer is quite easy and vast. Thermal convection is also simultaneously reduced this way. As the thermal conduction of air is much lower than that of solids, so thermal conduction of hollow fibers is reduced [48,49].

Aerogels possess thermal conductivity in different ways. Thermal conductivity via the aerogel core is expressed as follows:

$$\lambda_2 = \lambda_{\text{conv}1} + \lambda_{\text{cond}1} + \lambda_{\text{rad}1} \quad (10)$$

In aerogel, there is a cellular networking structure with pores diameter of tens of micrometers. These two factors suppress air circulation, thereby decreasing thermal convection. Air possesses the least value of thermal conduction as compared to solid structures. Aerogels also possess almost 99% porosity, thereby reducing thermal conduction. Aerogel porosity enhances its thermal properties and also prohibits all types of infrared radiation [50]. Hollow fibers can capture the aerogel precursor and also help to restrain air convection. Due to the above superior properties, aerogel behaves like a superior thermal insulating material with its microstructure and sheath. However, there are several factors that can modify its microstructure and sheath, like improvements in the design of the sheath and microstructure, enclosing air pockets in its structure, and further decreasing the pore size [51]. However, the volume ratio of the core microstructure and sheath should be uniform to tune all these characteristics. Aerogels are the best insulators because they do not favor all heat transfer modes. If the gas molecular free path diameter is more than its pore diameter ($Kn > 1$), the gas molecule will not strike with other gas molecules; rather it will strike with the walls. Due to this, thermal conductivity decreases. This effect is known as Knudsen effect. Knudsen equation is as follows [52]:

$$\lambda_g = \frac{\lambda_{g0}}{1 + \beta \cdot Kn} \quad (11)$$

Here, λ_{g0} is the thermal conductivity of the gas at standard conditions ($\lambda_{\text{air}} = 1/4 \text{ 26 mW m}\cdot\text{K}^{-1}$), β is a factor for the energy transfer between gas molecules and the surrounding cell walls ($\beta = 2$ for air) and Kn is the Knudsen number. The thermal conductivity of silica Aerogels granules and composites is evaluated by Lee's Disc method (ASTM C177-13). The apparatus consists of three plates made of copper ($75 \times 45 \times 3 \text{ mm}$) [53]. The heater is also connected with 5 levels of input power 1.18, 1.92, 3.16, 4.75, and 6.84 W. Thermal probes are fixed at first, second, and third copper plates. Basically, the silica aerogel granules are fixed between these copper plates at ambient temperature and pressure. The required time is 1–2 h after that thermal probe temperature is at a steady state [54].

Thermal conductivity is basically calculated from the following equation:

$$Q = (\lambda A_y) \frac{(T_2 - T_3)}{t} \quad (12)$$

In this equation, "Q" represents the quantity of heat flowing in watts; " λ " is the thermal conductivity having units $\text{W}/\text{K}\cdot\text{m}$. "A" is the area of the surface, and "t" is the required time. It was found that porosity and structural orientation highly affect thermal conductivity. It was also observed that thermal conductivity has a direct relationship with density. Heat transfer through conduction decreases in the same manner as density decreases, as shown in Figure 7b.

Thermal conductivity has an inverse relationship with porosity, as shown in Figure 7c. As porosity increases, it enhances the amorphous regions in the structure, which also hinders heat conduction. Heat conduction is very much decreased in amorphous regions because heat cannot find any trap states to flow through the material [55].

Thermal conductivity can be tailored using different precursors. TEOS is the most useful substrate; SS causes many impurities, whereas MTMS is also utilized for aging purposes. The effect of different substrates on density, processing temperature, porosity, and thermal conductivity is listed in Table 1.

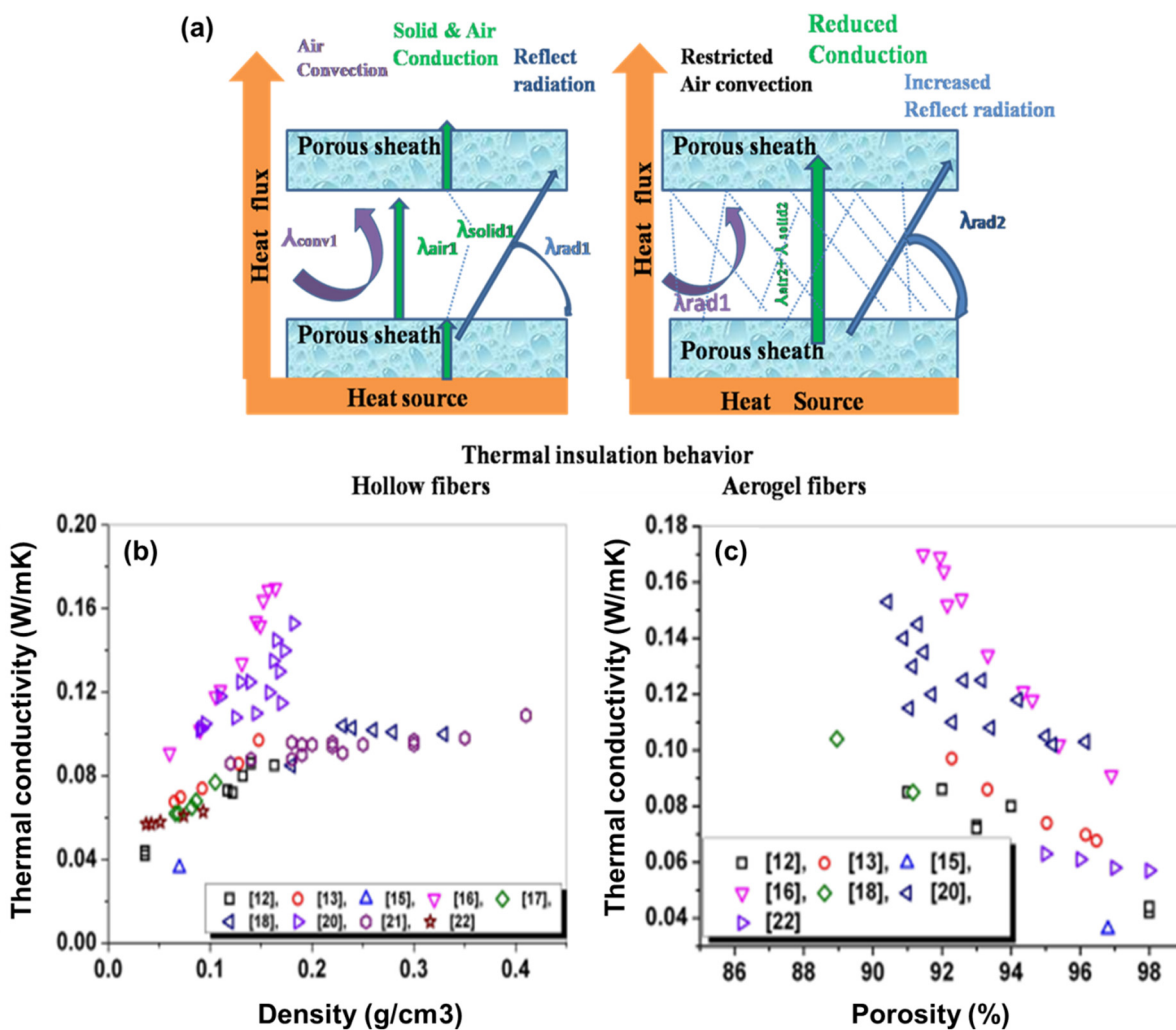


Figure 7. (a) Comparison between thermal insulation through hollow fibers and aerogel fibers; (b) Thermal conductivity with respect to density; (c) Thermal conductivity with respect to porosity. Reproduced from [56].

Table 1. Comparison of properties for different drying technologies [57].

Precursor	Drying Type	Thermal Stability °C	Thermal Conductivity	Porosity	Density	Ref
TEOS	APD	550	0.08–0.1	84.21–91.16	0.23–0.33	[58]
MTMS	SCD	480	0.09–0.098	----	0.1–0.35	[59]
MTMS	SCD	490	0.057–0.063	95–98	0.037–0.093	[59]
TEOS	SCD	300	0.068–0.099	92–96	0.06–0.15	[60]
TEOS	APD	200–520	0.042–0.086	91–98	0.036–0.163	[61]
SS	APD	320				[61]
SS	APD	325	0.091–0.170	92–96	0.152–0.06	[62]
TEOS	SCD	100–300	0.103–0.355	72–96.8	0.036–0.417	[62]

8. Heat Transfer Calculation

Many heat transmission techniques make use of composite systems, and some even combine conduction and convection. When working with these composite systems, it's generally easier to work with a U-factor or overall heat transfer coefficient. The U-factor is determined by a formula that is similar to Newton's cooling law [63]:

$$q = U\Delta T \quad (13)$$

q is the total heat flux density in units (Wm^{-2}). U is the overall heat transfer coefficient (Wm^{-2}K) whereas ΔT is the temperature difference. From Figure 8a, assuming one-dimensional heat transfer through the plane wall and disregarding radiation, the overall heat transfer coefficient can be calculated as follows:

$$U = \frac{1}{1/h_1 + L_1/k_1 + 1/h_2} \quad (14)$$

U is the overall heat transfer coefficient (Wm^{-2}K); K is the materials conductivity ($\text{Wm}^{-1}\text{K}^{-1}$); and h is the convection heat transfer coefficient (Wm^{-2}K) [64].

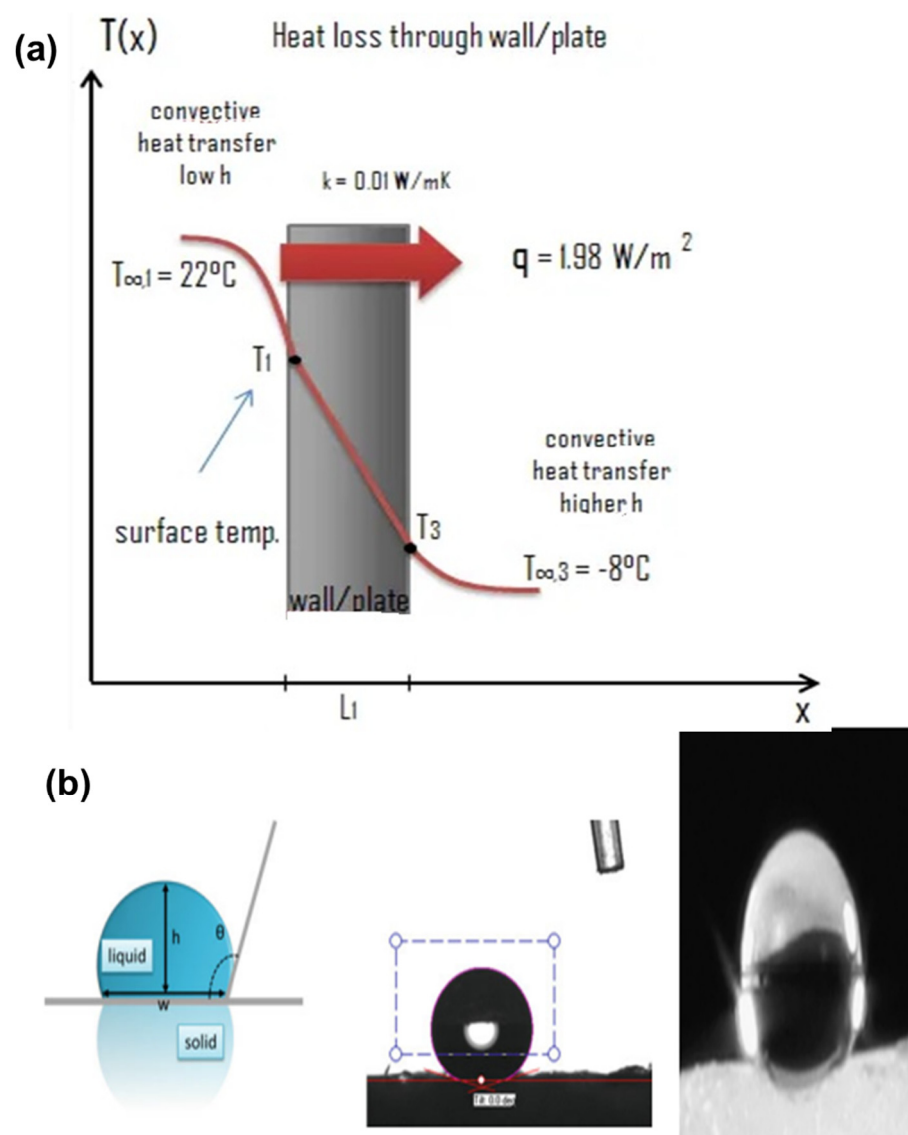


Figure 8. (a) Heat Transfer; (b) Hydrophobicity between different media.

9. Hydrophobicity

Aerogels can be hydrophilic or hydrophobic. Hydrophobicity and hydrophilicity depend on the substrate, precursor, silylating agent, and drying method. Hydrophilic aerogels did not get much emergence because when the water drop absorbs it, it scatters into the structure, colloids with the walls, and deforms the structure [65]. There was one main application of hydrophilic silica in drug delivery because of its hydrophobic character. Most of the applications fall under the hydrophobic nature of aerogels. Over 350 °C, the hydrophobicity of aerogel is converted into hydrophilicity due to oxidation. Hydrophobicity is basically the characteristics of the contact angle (θ) of a water droplet with an aerogel surface. It is the wetting of a solid by a liquid. When the liquid forms an angle at the three-phase boundary, the solid, liquid, and gas phases intersect, as shown in Figure 8b [66]. The contact angle is measured by the following equation:

$$\theta = 2 \tan^{-1} 2h/w \quad (15)$$

In the above equation, w is the width and h is the height of the water droplet. If the angle is less than 90°, liquid will wet the surface. Complete wetting occurs at 0°. Materials having a contact angle greater than 90° are called hydrophobic. For superhydrophobic, the contact angle should be greater than 150°. Contact angles are subclassified as dynamic and static angles [67]. When a droplet is standing on the surface and the three-phase boundary is not moving, dynamic and static contact angles are measured (Scientific 2015). Dynamic contact angles are referred to as advancing and receding angles when the three-phase boundary is moving [68,69].

10. Classifications of Aerogel

Aerogels are classified according to chemical nature organic, inorganic, or composite, and further classified mentioned in Figure 9. Classifications of aerogels on the basis of appearance, preparation method, microstructure, and chemical structure are shown in Figure 10.

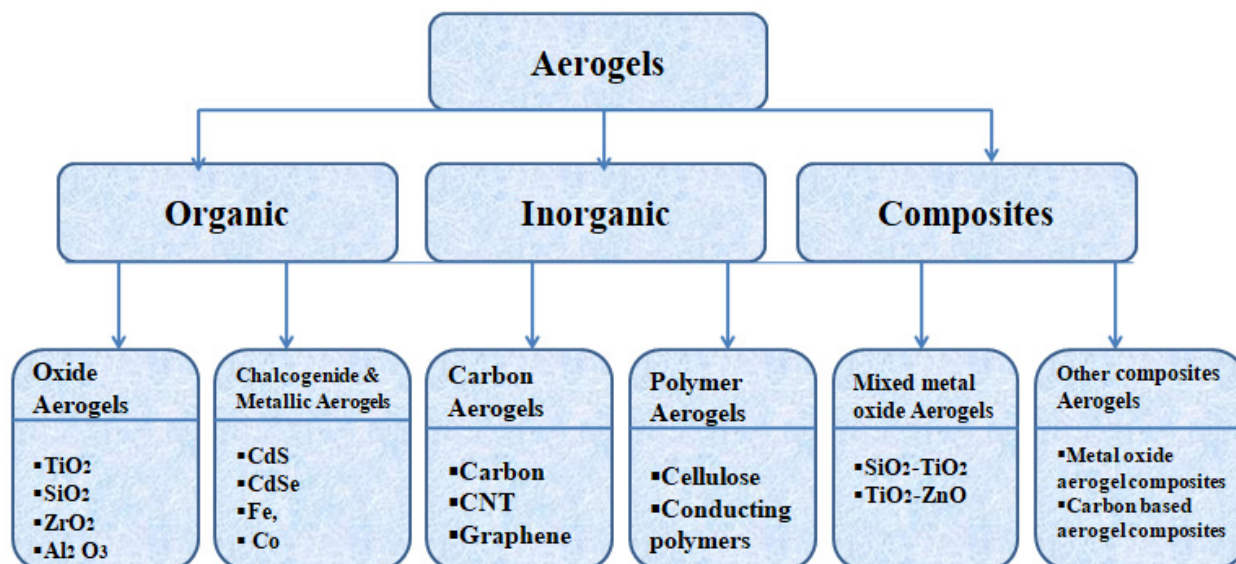


Figure 9. Aerogels classification. Open access, Reproduced from [70].

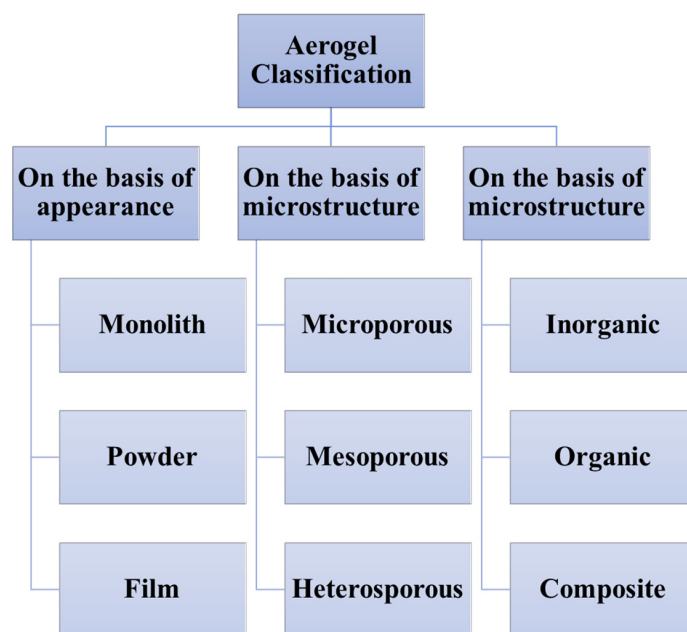


Figure 10. Aerogel classifications according to characteristics, Reproduced from [71].

10.1. Silica Aerogels

Silica aerogels are comprised of basic silica networking partial filler air packets, along with 3D networking structures. It has (-Si-) atoms at its backbone structure, forming siloxane bridges. Native silica aerogels cannot be handled alone and remain monolithic so there is a need to reinforce silica for enhanced mechanical properties (Figure 11). Silica aerogel properties are mainly affected due to their intrinsic fragility, thereby producing strains on the surface [72]. Scientists discovered many strategies, mainly to reduce its densities for high shock energy absorption. Low-density aerogels are highly preferred for bending and compression applications. For load-bearing applications, aging of wet gel is recommended, in which inorganic networks are formed, thereby increasing the strength of the final particles [73]. By this, the modulus of elasticity is also increased by a factor of two. Hybridization is also a good option for increasing mechanical properties by promoting the co-gelation of the silicon alkoxide with hybrid precursors such as poly (dimethylsiloxane) (PDMS) [74]. The gels formed by this are termed “ORMOSIL” (Organic modified silica) hybrids. Its flexibility is similar to rubber, but it can be elastically compressed up to 30% (by volume) with no damage [75,76].

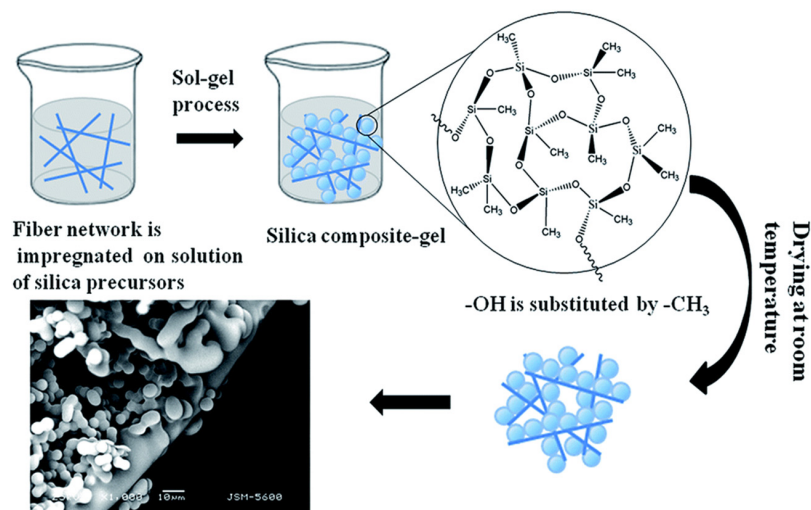


Figure 11. Silica aerogel synthesis and SEM morphology. Open access, Reproduced from [77].

10.2. Metal Oxide Aerogels

It is the most abundant class of aerogels structured with metal-oxygen bonds. These have unique characteristics; they behave as catalysts for chemical transformations and precursors for carbon nanotubes. Alumina oxide (Al_2O_3), zinc oxides (ZnO), titanium oxide (TiO_2), and iron oxide (Fe_2O_3) are major metal oxide materials used in this area. Their porosity ranges from 1 to 25 nm and possesses a low density of 0.06 g/cm^3 ; for $\text{Al}_2\text{O}_3/\text{SiO}_2$, the density is slightly higher, $0.54 \text{ g}\cdot\text{cm}^{-3}$, and porosity is varied between 77% and 96% [78,79]. These types of aerogels are prepared via the sol-gel route. In Figure 12, the hydroxyl group is formed by the reaction of metal aloxide with water. This step is known as hydrolysis. After this, aloxide is hydrolyzed partly, and then condensation occurs [80]. There may be a dehydration or dealcoholization reaction between aloxy and hydroxyl groups or with two separate hydroxyl groups. The nucleation rate is very low as compared to propagation to avoid agglomeration.

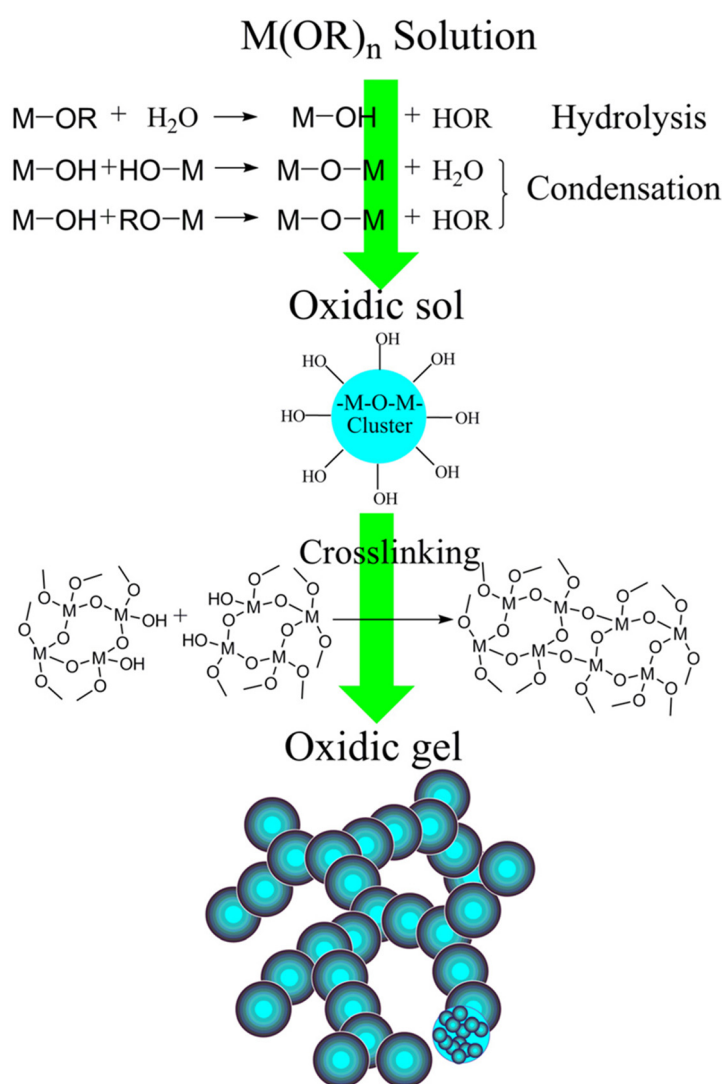


Figure 12. Metal oxide aerogels. Open access, Reproduced from [15].

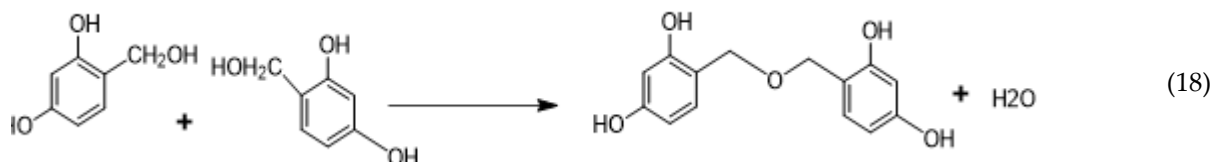
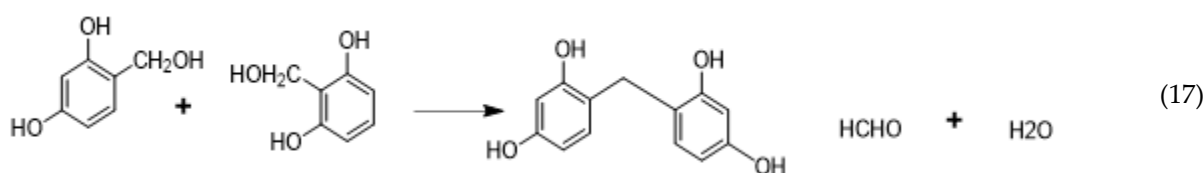
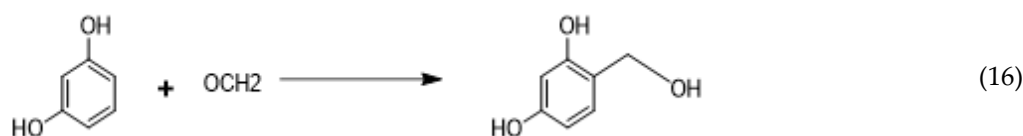
This also affects the cluster size as the lowest nucleation rate also results in smaller particle sizes. Growth rate is more related to diffusion rate and degree of supersaturation. At the growth stage, the hydrolysis rate is important. A high hydrolysis rate leads to the formation of supersaturated solution so there is a need to decrease it. To decrease the hydrolysis rate, the reaction should be catalyzed under an acidic or basic environment to get a stable colloid [80].

10.3. Organic and Carbon Aerogels

Organic aerogels basically contain cellulose and resin in their backbone structure. Organic aerogels are synthesized with both monomeric and polymeric precursors such as polyvinyl chloride, phenol melamine, polymeric isocyanate, phenol-furfural cresol formaldehyde, and melamine-formaldehyde. Precursor is carefully chosen as end product applications are certainly dependent on it. These types of aerogels are highly recommended for membrane-based gas separation, acoustic insulators, dielectrics, and catalyst supports [81,82].

Its polymerization includes the following two steps:

1. Addition reaction between formaldehyde and resorcinol to form hydroxymethyl resorcinol monomers (Equation (16));
2. $-CH_2-$ or $-CH_2OCH_2-$ bridging polymerization between monomers, producing formaldehyde or water (Equations (17) and (18)).



When clusters crosslink, gelation occurs. RF clusters are the result of continuous polymerization. These are used for high mechanical strength applications [51,83].

Carbon aerogel (Figure 13) is a branch of organic aerogel possessing a higher porosity rate and interconnected clusters of carbon nanoparticles having 3–20 nm diameter. To obtain carbon aerogels from organic aerogels, temperatures above 600 °C are required for carbonization or pyrolysis [84]. Additionally, there should be an inert gas atmosphere (nitrogen, helium, or argon). These are highly porous, graphite-based aerogels. Carbon aerogels are preferred for electric storage and hydrogen production devices because of their higher porosity and corrosion resistance. Carbon aerogels were further modified into diamond aerogels by laser-heated diamond anvil cells. These are superactive media for catalyst support and acoustic insulators [85–87].

Zhang et al. published a rather novel method for synthesizing graphene aerogel in 2011. L-ascorbic acid is used to self-crosslink graphene oxide, which is subsequently dried [19,88]. The benefit of this approach is that no extra pyrolysis treatment is required. Carbon nanotube (CNT) aerogel is another intriguing type of carbon aerogel. In 2007, it was originally produced by sonicating CNT into a surfactant solution, followed by gelation and drying. Polyvinyl alcohol could improve aerogel even further [89]. In 2009, Aliev et al. reported synthesizing CNT aerogel fibers by extracting them from multiwall nanotube forests' straight sidewalls [90]. Since its raw material (CNT forests) was created by catalytic chemical vapor deposition, it differs from practically all previous aerogels. Another "dry synthetic method" for creating carbon-based aerogel (aerographite) involves chemical vapor deposition of nanostructured graphite onto ZnO network templates, hydrogen

atmosphere reduction of ZnO to metallic Zn, and high-temperature sublimation of Zn. The end product has an extremely low density [91].

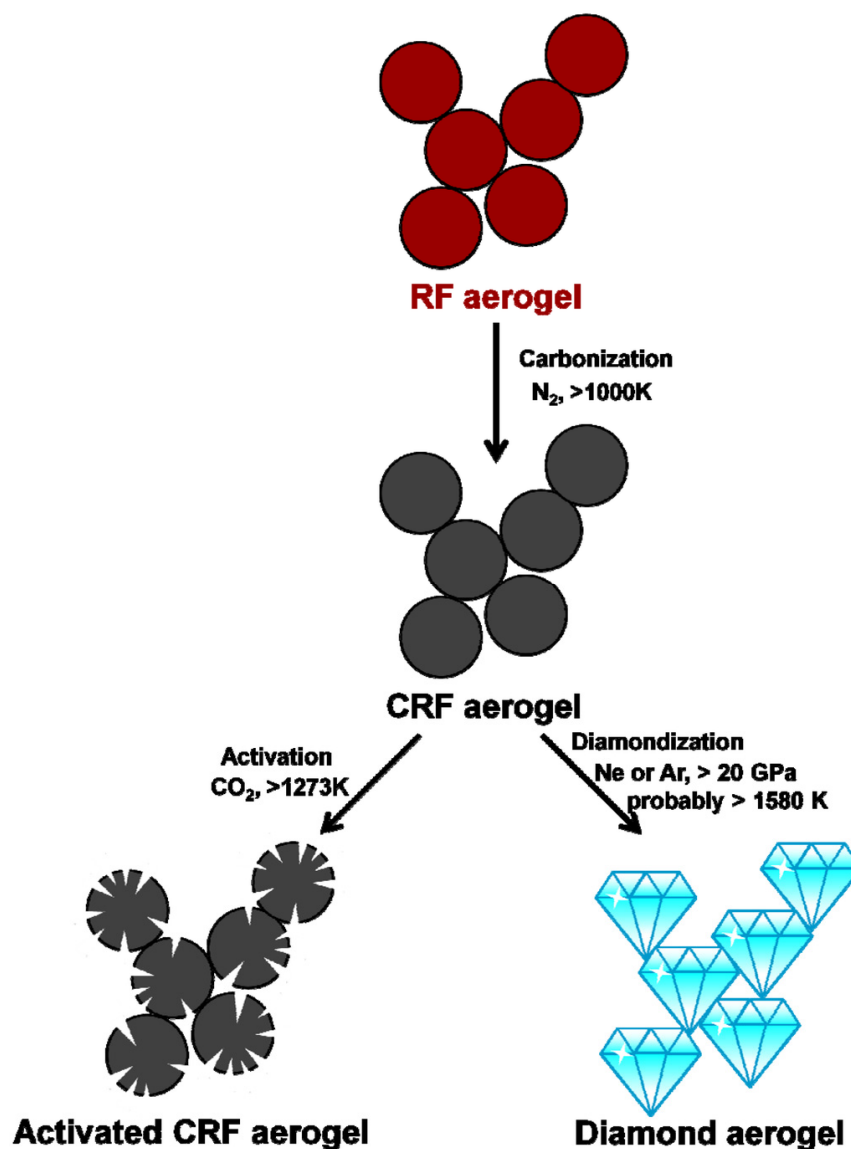


Figure 13. Carbon aerogels. Open access, Reproduced from [15].

There are some additional agents, like biopolymers, metal clusters, and some organic molecules, that can be added into SA matrix for enhanced mechanical properties. Powders, beads, rods, fibers, blankets, and boards are all examples of SA-TIMs. It has incredible potential to meet the current needs of fire prevention, thermal insulation, adsorption properties, medical, aerospace, and home building sectors [91], due to its unique combination of the above-mentioned properties. There are still numerous technical challenges, particularly in mass production and distribution.

10.4. Hybrid Aerogels and Composite Aerogels

The most researched hybrid aerogels incorporate both inorganic and organic phases, nanoparticles, and cross-linked polymers into the gel matrix. They are then reinforced with fibers and filler to create interpenetrating networks [92]. These aerogels were acquired in order to enhance their processing as well as their mechanical, physical, and other qualities. The co-pyrolysis of soft fibers such as polyacrylonitrile (PAN) with an RF aerogel matrix yields composite aerogels as carbon fiber-reinforced composites. The aerogels' toughness,

strength, and thermal conductivity are all increased by this technique [93]. The aerogels' toughness, strength, and thermal conductivity are all increased by this technique. Examples of this kind of aerogels include cross-linked polymer aerogels, functional nanocomposite aerogels that contain metal or metal oxide nanoparticles in the aerogel matrix with special electrical, catalytic, optical, and magnetic properties, and nanocomposite carbon aerogels containing carbon nanotubes (CNT) [94,95]. Other examples include carbon aerogels containing nanoparticles of various metals, including Cr, Zr, Mo, Fe, W, Co, Ni, Pd, Pt, Cu, and Ag, as well as silica aerogels containing transition metal oxide nanoparticles, such as NiO [96], ZnO [97], TiO₂ [98], Al₂O₃ [99], CuO, and CoFe₂O₄ [100,101].

10.5. Carbon Nanotube Aerogels

Critical-point drying and freeze-drying were used to make carbon nanotube (CNT) aerogels from aqueous-gel precursors, according to M.B. Bryning et al. [102]. The CNT aerogels were robust and conducted electricity to enhanced electrical characteristics. Small amounts of polyvinyl alcohol can be used to strengthen the aerogels. This type of aerogel can withstand 8000 times its weight. Because of their high strength-to-weight and surface-area-to-volume ratios, these materials frequently offer unique features. These aerogels were created by constructing a free-standing, three-dimensional network of carbon nanotubes in the air directly from CNT networks in suspension. Because CNT aerogels can be back-filled with a polymer or other material, they can be used as the foundation for composite structures made of a wide range of materials [103].

10.6. Polyurethane Aerogels

Polyurethane aerogels are a type of aerogel material that is derived from polyurethane polymers. They belong to the broader category of polymer-based aerogels and offer unique properties and applications due to their composition and structure. Polyurethane aerogels are typically formed through a sol-gel process similar to other types of aerogels [104]. The process involves creating a solution (sol) of polyurethane precursors, often consisting of diisocyanates and polyols. These precursors undergo a polymerization reaction to form a three-dimensional network structure within a liquid phase. A solvent exchange and drying process, often involving supercritical drying, removes the solvent while preserving the porous structure, forming polyurethane aerogels [105].

11. Aerogels Photocatalysts Synthesis

Aerogel photocatalysts can currently be made using two different methods: direct synthesis using a molecular-based sol-gel strategy, assembling using nanoscale units as templates, and immobilizing photocatalysts in aerogel frameworks. The former is influenced by traditional sol-gel chemistry, which uses molecular precursors, condensation, and hydrolysis to create SiO₂ aerogels. Only a few different types of metal oxides, including SiO₂, TiO₂, Al₂O₃, and ZrO₂, as well as chalcogenides (ZnS, WS_x, and GeS₂), are present in the molecular precursor [106]. Additionally, the prepared aerogel has generally low crystallinity. It is preferable to use the assembly method to investigate high-crystallinity aerogels. The range of aerogel photocatalysts has been greatly expanded by nanocrystalline colloids such as chalcogenides (CdS, CdSe, PbS, ZnS), metal oxides (MnO₂, Fe₃O₄, SnO₂), metal-free compounds, and their composites. Recent advancements in this subject have been made possible by the construction of 1D and 2D crystalline building components like nanowires and nanosheets. More potential photocatalytic applications are provided by the availability of these premade building blocks to attain the requisite characteristics prior to producing aerogels [44].

Immobilization of Aerogels as Photocatalysts

Although directly synthesized aerogel photocatalysts have been extensively studied, only a small number of photocatalysts can be converted into aerogel photocatalysts using the sol-gel or self-assembly processes, severely restricting their practical application [107].

Immobilizing photocatalysts on the already-prepared aerogel framework to create composite aerogel photocatalysts has thus attracted a lot of attention recently in an effort to streamline the fabrication process and increase the variety of aerogel photocatalysts. In order to create composite aerogel photocatalysts, it should be remembered that practically all photocatalysts can be added to the aerogel framework as shown in Figure 14 [108]. Additionally, the composite aerogel photocatalyst has the benefits of the aerogel framework as well as the ability to operate as a photocatalyst. When a photocatalyst is exposed to light, photons are absorbed, and excitons are generated. Higher excitons can enhance photocatalytic activity by increasing the probability of electron-hole separation and, thus, the production of ROS. These excitons can then be separated into their constituent electrons and holes, which can participate in redox reactions with adsorbed molecules on the photocatalyst surface. This photocatalysis in the mobile phase facilitates the generation of ROS and increases the efficiency of the process [109]. Compared to the mobile phase, the photocatalysis is slower in the passivated state, i.e., coated on fabric. However, the easier recovery of active materials and careful design, as well as optimization of the photocatalyst's properties with minimal secondary pollution, make the proposed strategy closer to practical applications [110,111].

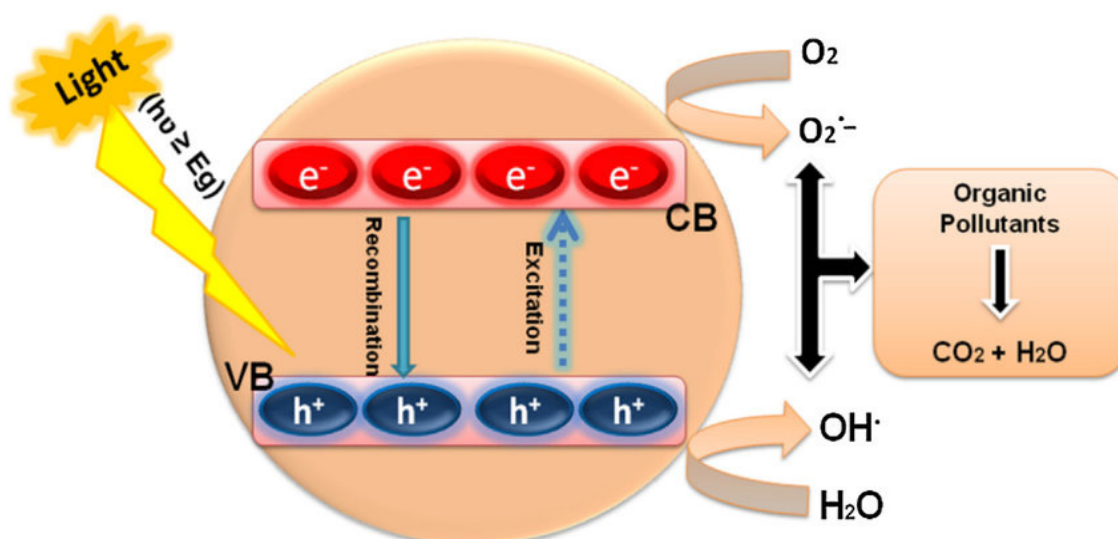


Figure 14. Aerogels photocatalysis mechanism.

12. Preparation Process

To synthesize the aerogel structures, it is quite essential to control the microstructure for preparation of silica aerogel thermal insulation microstructures SA-TIMs because their end application is strictly based on microstructure and processing parameters. Generally, SA-TIMs synthesis includes the following three strategies, as also shown in Figure 15.

12.1. Solution-Sol Transition

Nanoparticles of the sol formation occurred; precursor solution is prepared at any solvent and may be catalyzed by hydrolysis or through other assisted reactions, and finally, aloxysilanes are added [32]. The required solvent should be properly miscible and able to prepare the homogenous mixture. Preferred solvents are ethanol, alcohol, acetone, tetrahydroflourane, etc. The phase diagram of aloxylane-water-solvent is shown in Figure 16a. If the solvent is alcohol, it can decrease the hydrolysis rate by esterification reaction. The choice of solvent is necessary to synthesize the desired product. If the solvent is not able to dissolve the required amount of aloxysilanes, it can cause agglomeration [112].

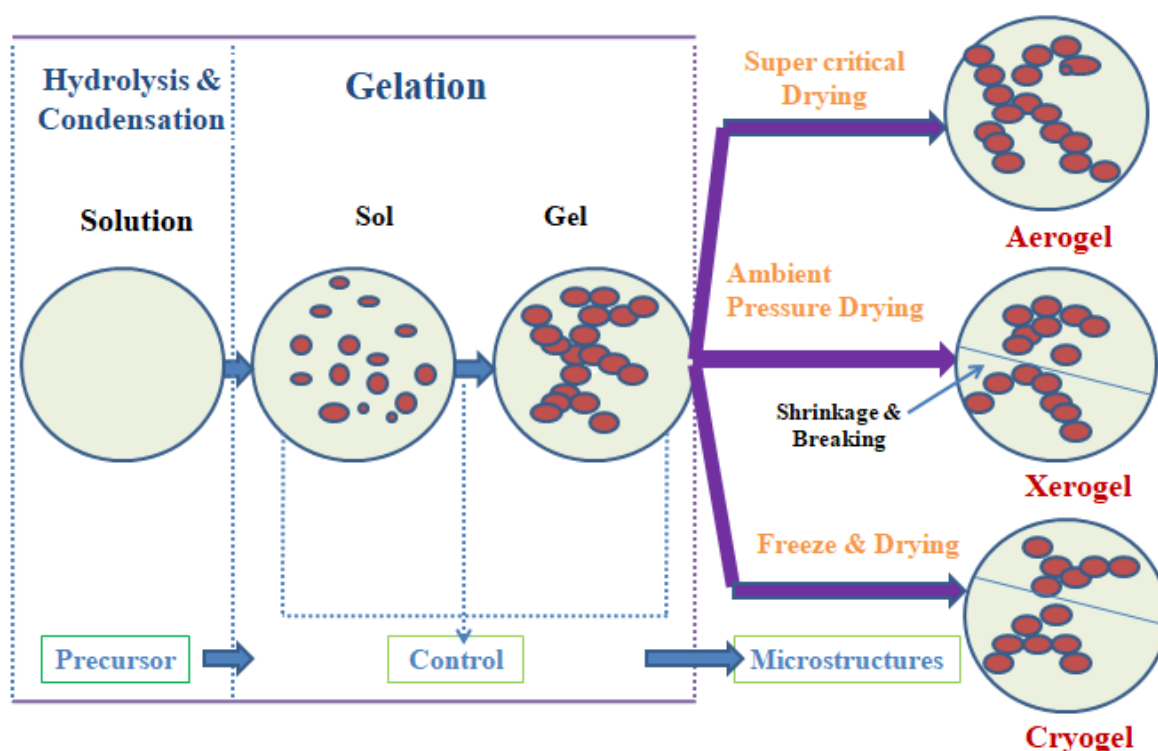


Figure 15. Synthesis strategies of silica aerogels.

12.2. Sol-Gel Transition (i.e., Gelation)

In this stage, the sol is converted into a gel by forming a 3D networking structure cross-linked with each other to form a metastable state. It can be chemically of any nature or physical (temperature, pressure, pH). This state is achieved by uniform stirring for 5 to 6 h with optimized parameters. Stirring rate and temperature are two confined parameters affecting its shape and structural parameters. Uniform stirring is necessary to avoid agglomeration [113].

12.3. Gel-Aerogel Transition (i.e., Drying)

Now sol-gel solution needs to be dried to replace the water and alcohol particles by air without cracking and subsequent drying of the dried aerogel. The existing nanoporous microstructure should not be collapsed; otherwise, it will deteriorate the final properties. Mainly, there are three techniques for drying the sol-gel [36,114].

- i. Supercritical drying, in which the sol-gel is dried above the critical point of solvent without the capillary effect of surface tension between the vapor and liquid phases, leads to uniformity in the structure, higher porosity, and optimal textural characteristics [115]. Basically, this drying is generally used to convert the gels into Aerogels as shown in the Figure 16b. In the initial stage, wet gel is dried and expanded liquid is formed due to increased capillary movements of atoms [115]. Now its atoms are more interactive with each other. In the next step, a supercritical fluid mixture is formed which has the ability to effuse through a solid like a gas. At this stage, almost 50% of the solvent is removed. In the next stage, diffusion-controlled drying proceeds in which solvent is removed up to 98% without the action of capillary forces. Now the wet gel is completely converted into aerogel.
- ii. Ambient pressure drying, in this drying, is achieved with silylation treatment thereby increasing the structural strength. Capillary forces are much reduced during solvent evaporation. It can reduce the production cost and safety risks [116].
- iii. Freeze-drying, in which the solvent is evaporated by decreasing the wet gel temperature below the crystalline temperature of the solvent, like sublimation. Most

xerogels and cryogels are produced by this drying [117]. It allows complete removal of solvents while achieving 95% porosity without any shrinkage. This process also has some disadvantages, like health hazards and irreversible shrinkages. The network of a silica cryogel takes a considerable aging period to solidify, and the network is easily damaged by the crystallization of the solvent in the pores. As a result, the majority of silica cryogel products are powders, and producing monolithic silica cryogels is extremely challenging [118].

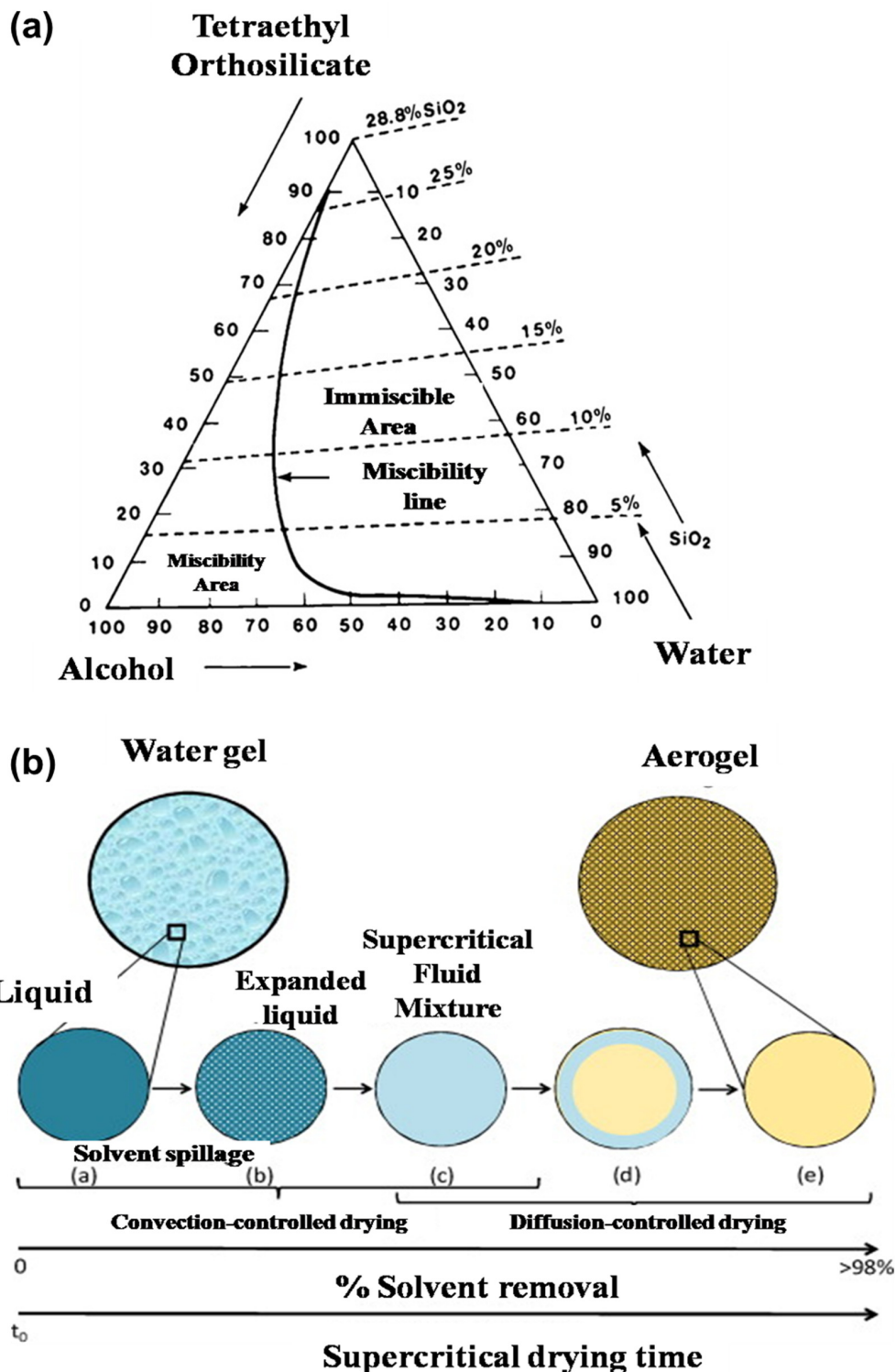


Figure 16. (a) Phase Diagram of aloxylane-water-solvent, (b) Supercritical drying.

13. Design Principles

There are some challenges of SA-TIMs, like enhancing hydrophobic functionalities, strong scalability, high-temperature performance, and mechanical strengths for desired aspects. There are many factors like material and process design, synthesis route, composition, and environmental factors that ultimately affect its performance, as shown in Figure 17. If we have a simulative control of the microstructure and morphology of nanoparticles, it will enhance thermal conductivity and mechanical strength. Some other properties like density, processability, and temperature resistance can also be tuned by optimizing synthesis parameters [119,120].

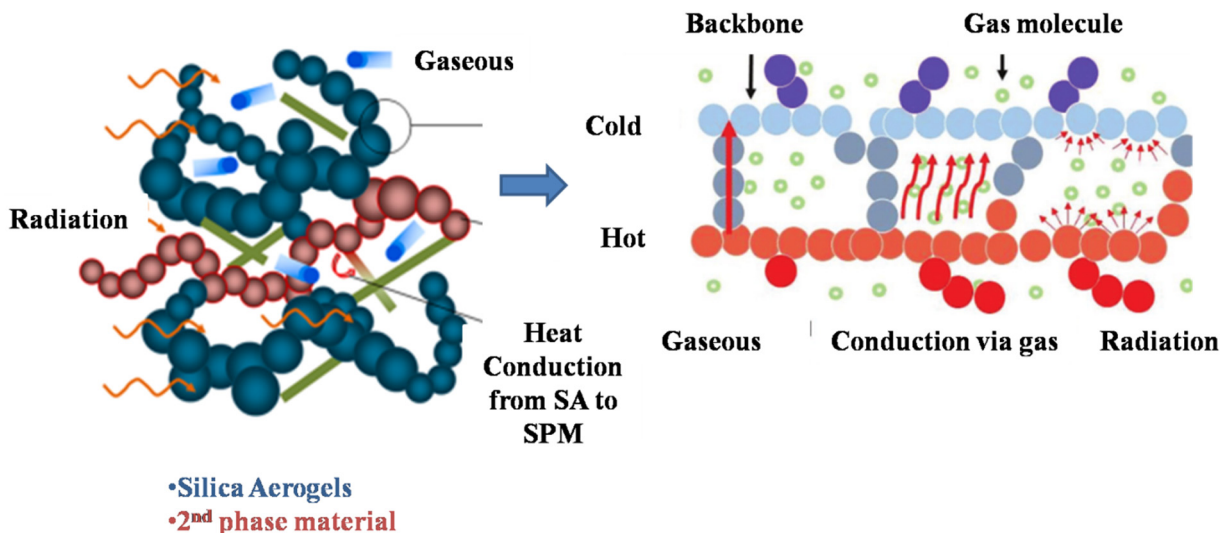


Figure 17. Design principles.

Thermal transportation of aerogel includes heat conduction through a solid backbone, heat conduction with gas molecules, and then there occurred thermal radiation through the backbone structure. Thermal conductivity basically depends on the type, composition, shape, and hybrid structure of SA Skelton and nanoparticles. Morphology, packing arrangement structure, and structure ordering also have as strong impact on thermal conductivity [121,122]. If there is an addition of second phase material in the structure, it exhibits the radiation collapse at the structure. If the surrounding air produces a microclimate with an even temperature difference, a net amount of heat flows because of the air. The thermal conductivity of SA-TIMs is basically the sum result of solid, gas, and radiation conductivity as follows:

$$(\lambda_{total}) \text{ of SA-TIMs} = (\lambda_{solid}) + (\lambda_{gas}) + (\lambda_{rad}) \tag{19}$$

Thermal conductivity of solid is limited due to porous and nanoporous structure so it does not affect highly. Thermal conductivity of radiations is controlled by porosity, pores sizes, and refracting and reflecting surfaces [123]. The remaining space is obviously filled by gas and the thermal conductivity of gas is as:

$$\lambda_{gas} = \lambda_{g0} / (1 + \alpha T / \delta P) \tag{20}$$

In the above equation T, P, and δ represent the temperature, pressure, and pore size of gas, respectively, whereas α is a specific constant.

SA-TIMs λ_{tot} depends on all these external and internal parameters: morphology, presence of side chain, functional atoms, weaker or stronger bonds, pendant group, as well as segments [122,123]. Due to the difference in water vapor pressure at the surface and in the surroundings, moisture is exchanged between the two surfaces. The net amount of moisture exchange between these two surfaces affects vapor pressure as well

as thermal conductivity [124,125]. Furthermore, during the service life of SA-TIMs, vapor phase transport (convection and diffusion), liquid phase transport (wicking), heat transfer (convection, conduction, and radiation), liquid evaporation and condensation, and sorption/diffusion of water vapor and liquid through the solid phase occur. Because water vapor (0.025 W/(m·K)) has a lower heat capacity than water (0.620 W/(m·K)) and ice (2.220 W/(m·K)), reducing the number of adsorption sites (Si-OH) and siloxane (Si-O-Si) on the surface is critical [126,127].

14. Drying Technologies for Aerogels

Different drying technologies of aerogels i.e., ambient drying, freeze drying, supercritical drying parameters, conditions, limitations, costs, and preparation steps are mentioned in Table 2.

Table 2. Drying Technologies comparison.

Drying	Conditions	Preparation Steps Prior to Drying	Limitations for the Gel Matrix	Main Energy Costs/Risks
Ambient drying	<ul style="list-style-type: none"> Room T Ambient P 	Hydrophobization of the matrix is essential	Not preferable for hydrophilic and fragile matrices. Density > 0.1 g/cm ³ achieved	Low-energy cost, safe and less hazardous.
Freeze drying	<ul style="list-style-type: none"> P < 100 mBar −70 °C < T < −20 °C 	Structure compaction, use modifiers.	Pores are somehow destroyed. Density below 0.03 g/cm ³	High-energy cost, because of low-temperature batch process
Direct supercritical drying	<ul style="list-style-type: none"> T > 100 °C P > 30 bar 	Direct conversion of solvent to critical parameters. No solvent conversion.	Side reactions occur Temperature > 100 °C is not suitable with organic gels.	Moderate-energy cost, toxic
Super critical drying by CO ₂ extraction	<ul style="list-style-type: none"> P > 74 bar T > 31 °C 	Hydrogel solvent exchange occurs, so solvent should be compatible with CO ₂ .	CO ₂ /solvent transportation affects the properties	Energy cost is high because of compressed CO ₂ , lesser explosion risks

15. Aerogel Fibers

Producing aerogel-based fibers with unique properties like high porosity, lighter weight, and optimum density has been of scientific interest for a century. These fibers possess promising applications in hygiene products, drug deliveries, and filter materials [128]. Cellulose-based aerogels are synthesized with the dissolution of cellulose into suitable media like urea solution, sodium hydroxide, or any other ionic liquids. After this washing is performed before coagulation, and then drying is performed with any of the special drying methodologies, i.e., supercritical drying, freeze drying, ambient drying, etc. [90,129].

The first cellulose-based aerogel was reported by Tan et al., in which cellulosic aerogel was synthesized by salt hydrate as a unique dissolving agent. Ester with toluene-2,4-diisocyanate was a crosslinking agent. In this unique method, dissolution was carried out with Ca(SCN)₂ because of a similar coordination number. Toxic cyanates are also avoided in this technique. By dissolving Ca(SCN)₂ salt hydrate, porous aerogels were synthesized with gelation, coagulation, and supercritical drying [130]. Different ratios of cellulosic content up to 6% were added, and their properties were compared. In this way, 3D structures of cellulosic fibers at the nanoscale are achieved with envelop density from 0.5 to 6 wt% having cellulosic content between 0.009 and 0.137 g/cm³. The surface area ranged from 120 to 230 m²/g calculated by BET. Synthesized aerogels showed excellent thermal conductivity as well as mechanical strength at room temperature [131]. Synthesized aerogels obtained by coagulation, washing, and extrusion are also shown in the following Figure 18. It was found that the optimum extrusion range is 95–110 °C. SEM images of monolith

fibers are also shown to have a pore size of 10–100 nm and a diameter range of 10–25 nm. Both monolith and micro-extruded fibers have the same morphology except core structure difference. This difference is due to evaporation in the coagulation bath whereas the melt solution submerged into the regeneration bath. The fibers' unique architecture, which includes a meso and macroporous structure constructed at the top of a nanoporous network, opens up new application possibilities [132].

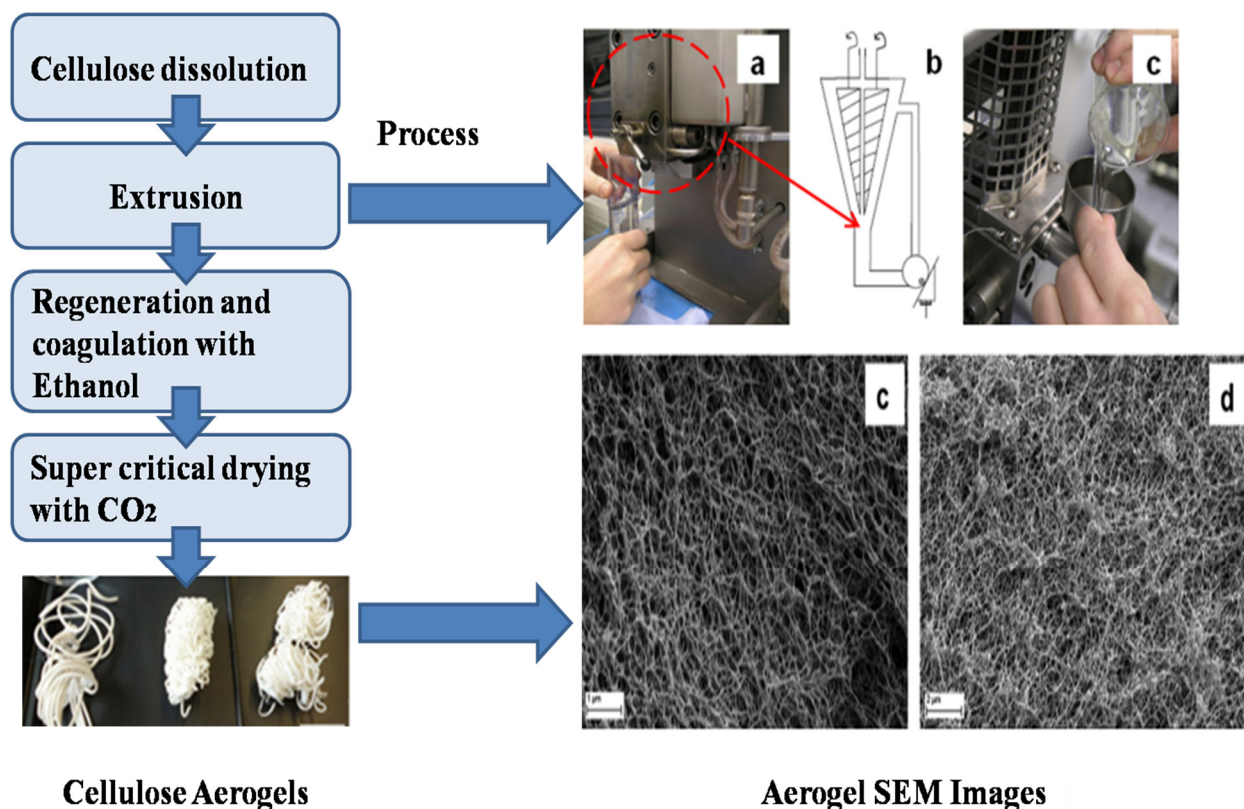


Figure 18. Aerogel fibers (a–c) Synthesis routes and design principles, (c,d) SEM morphology. Reproduced from [129].

Porous CA/PAA-wrapped SF aerogel fibers were synthesized and reported for high thermal insulation and high mechanical properties in applications [133]. Silk fibers were degummed, and dissolution gel was prepared. Then, the silk fibers were added into dialysis bag for preparation of silk fiber aqueous solution. At the final stage, freeze-drying process was performed. The CA/PAA hollow fibers having porous sheath not only possess high mechanical properties but also facilitate the formation of SF aerogel core. These also possess high porosity (86%), low density (0.21 g/cm^3), and high tensile strength ($2.6 \pm 0.4 \text{ MPa}$). Additionally, it is suitable for thermal insulation in both hot ($100 \text{ }^\circ\text{C}$) and cold ($-20 \text{ }^\circ\text{C}$) conditions. Thermal insulation properties can be tuned by core and sheath proportion and by numerically tuning other parameters. As a result of the delicate core–shell structure of aerogel fiber, it offers a new way to manufacture high-performance wearable thermal insulation materials, as shown in Figure 19.

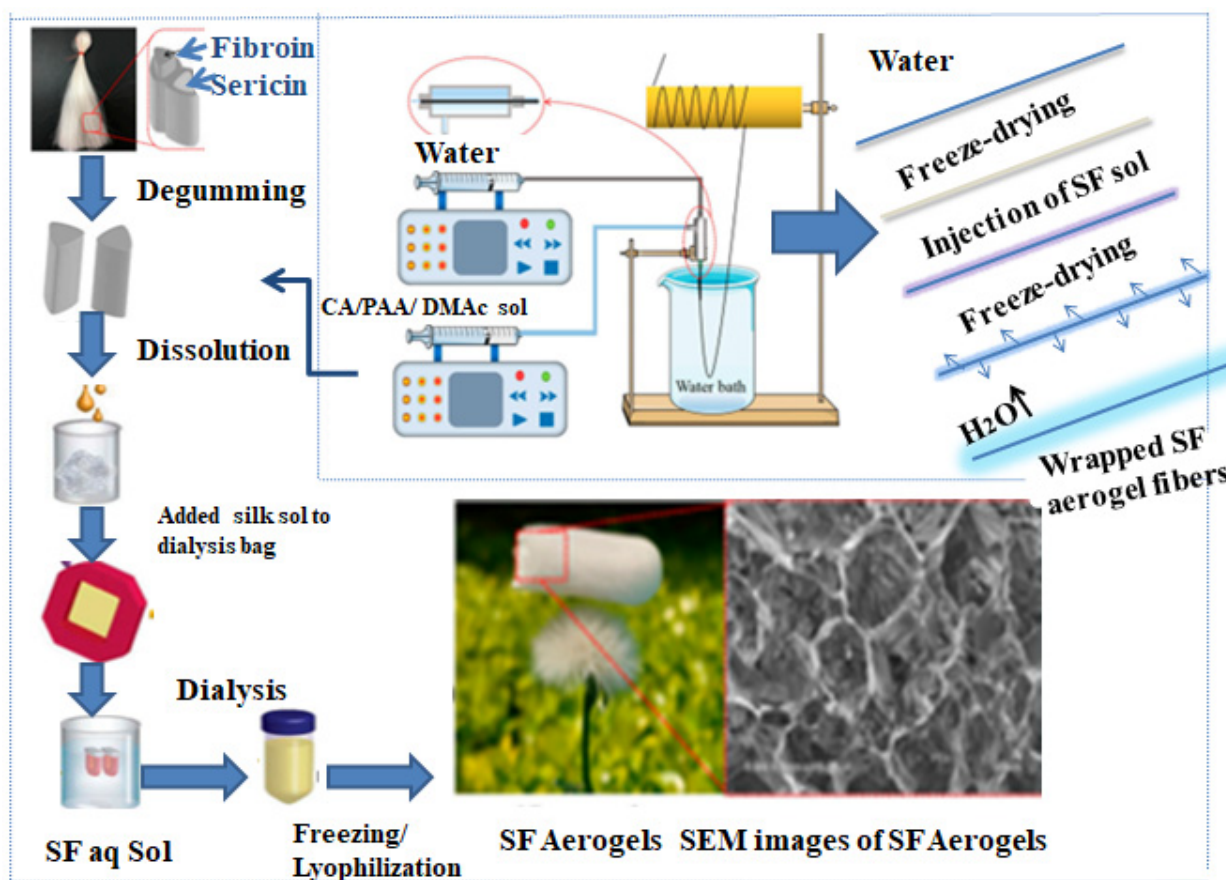


Figure 19. Aerogel fibers synthesis, Open access, Reproduced from [130].

16. Aerogel Fabrics

Aerogel fabrics (woven or non-woven) are manufactured to have high insulation and comfortable properties. Cellulosic or synthetic fibers are woven or non-woven together to assemble aerogel fabrics. Different synthetic or natural fibers were spun on an industrial scale by a compact melt spinning machine and subsequently processed into nonwoven fabrics on a laboratory-scale needling line, and sound absorption properties of blankets made of silica aerogel/polyester (PET) were examined [134]. The silica aerogel blankets were made by synthesizing silica aerogel on nonwoven fabrics in situ using a two-step tetraethoxysilane sol-gel technique and drying at ambient pressure. Various synthesis parameters were employed to generate aerogel particles with varying pore structures and characteristics [135,136]. As coarser fibers are used, there are fewer fibers per unit area and wider pores [137]. Figure 20 shows SEM micrographs of the nonwoven textile structures and aerogel blanket samples synthesized by nanofabrication. The SEM images clearly revealed the effectiveness of nanoaerogels on fibers. These coated fibers show enhanced thermal and heat regulation properties by providing sufficient moisture management capability to the wearer. As previously mentioned, the μ CT device used for this study has a resolution of 1–3 μ m. Therefore, this technique cannot be used for the characterization of aerogels in the internal structure of blankets [137,138].

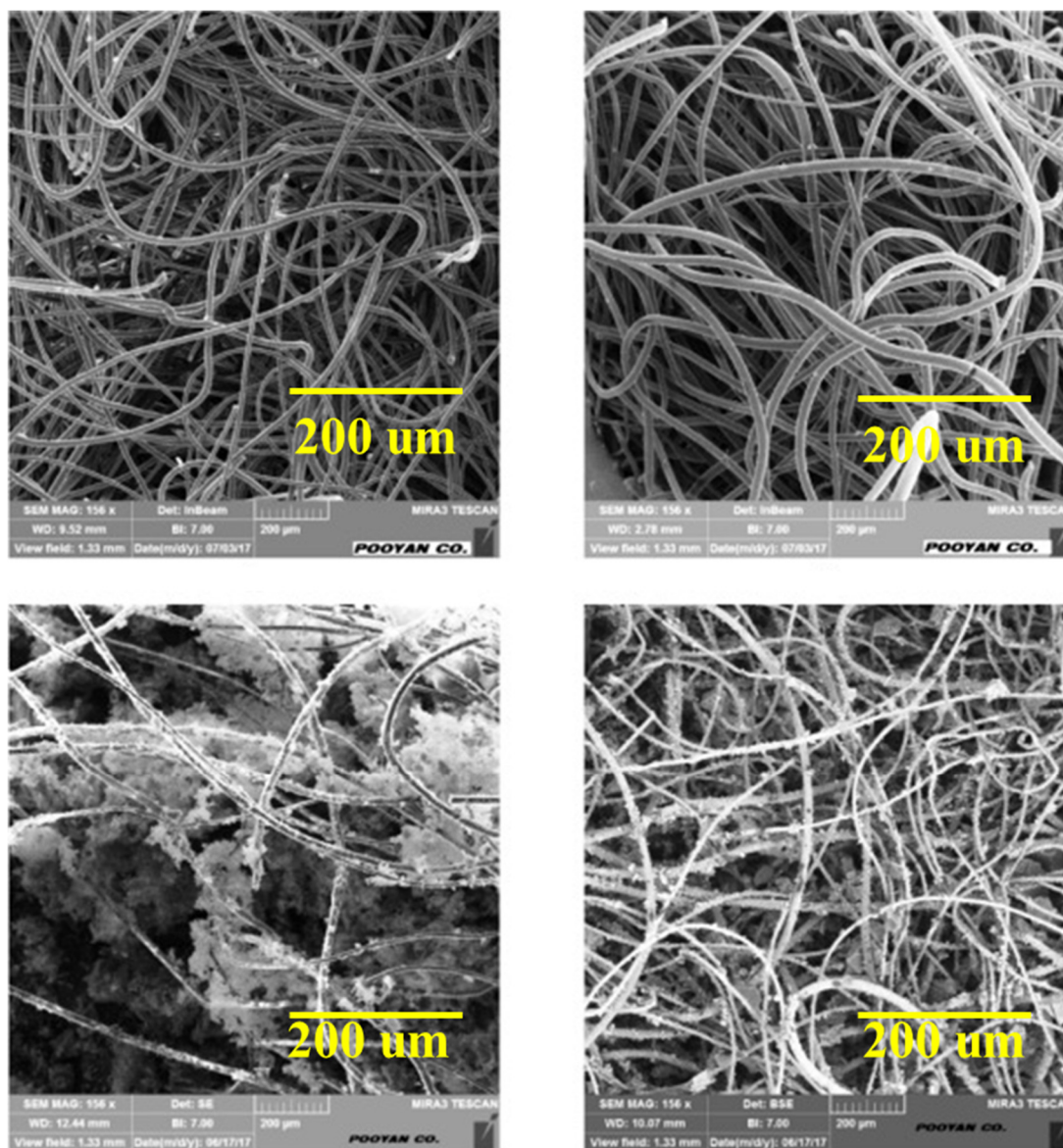


Figure 20. SEM images of neat nonwoven fabrics and aerogel blankets. Reproduced from [139].

The thermo-physiological comfort of a newly created fabric, which could be used for firefighter protective equipment, was discussed [140]. Super hydrophobic silica aerogel nanoparticles were incorporated into a 65/35 wool-aramid blended fabric to create thermally comfortable garments [141]. The performance of air, moisture, and heat transport was then used to assess thermo-physiological comfort. It has been discovered that a 2% aerogel nanoparticle coating can boost thermal resistance by up to 68.64% and reduce air permeability by up to 45.46%, while a 4% aerogel coating can reduce air permeability by up to 61.76%. The aerogel-coated fabric's moisture management properties have also been examined and described in depth [142]. The coating thickness has a positive effect on moisture transportation and overall moisture management, in conclusion. Again, the next-to-skin layer coated with aerogel and the outside layer coated with aerogel had different effects on the identical fabric. When the coating is applied to a surface that is near the skin, it has been found that the coated fabric behaves more like a moisture management fabric [143].

Using an acrylic glue, varying amounts of "NANO GEL" (superhydrophobic aerogel nanoparticle from Cabot) were applied to a 65/35 wool/Aramid blend fabric that weighs around 230 g/m². 2%, 4%, and 8% aerogel-coated fabrics were created with coating pastes

that ranged in viscosity from 20,000 to 30,000 centipoise as shown in Figure 21. After coated fabrics were cured for 10 min at 105 °C, their thermophysiological characteristics were examined [144].

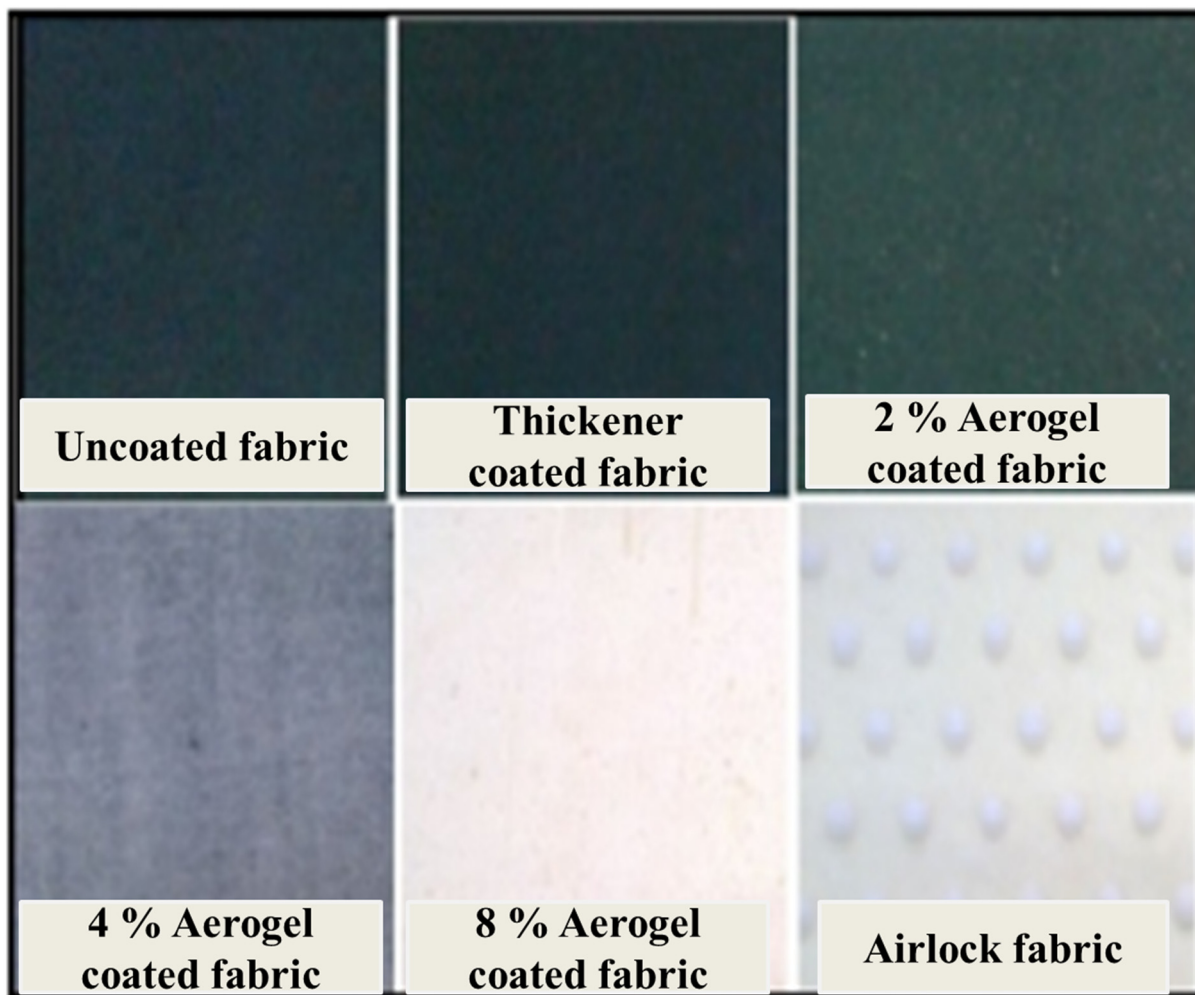


Figure 21. Aerogel coated fabrics microscopic images. Open access, Reproduced from [144].

In order to increase the wearer's thermophysiological comfort, the research looked into the potential use of aerogel in firefighter protective gear. The ability of aerogel-coated cloth to transmit heat, moisture, and air was examined in terms of thermophysiology [145]. These three qualities are thoroughly discussed [144]. The test results can be summarized as follows: the aerogel-coated fabric has good air resistance, the right coating thickener can reduce the hydrophobicity of the aerogel and the base fabric, improving the ability to manage moisture, and the aerogel-coated fabric provides better thermal insulation. In addition to being thermally insulative, aerogel can also significantly resist airflow, according to recent studies [146].

These two taken together show a technique for making textiles for clothing that offer thermally better insulation for a variety of uses in extremely hot and cold weather. Aside from the encouraging results, the research was hampered by a few inevitable limitations brought on by the short time restriction, such as the fact that not all varieties of made-up cloth samples had their heat resistance evaluated [147]. Again, the moisture management tests conducted call for a further in-depth investigation of several coating types with different Aerogel and thickener compositions on different fabric structures in the border range. However, the report offers general recommendations for further study on the use of Aerogel in protective apparel, based on successful research outcomes [148,149].

Figure 22 also shows that when a coating of 2% aerogel paste was applied, the aerogel particles did not completely cover the surface, whereas a coating of 4% showed partial coverage. The aerogel powder thoroughly coated the fabric surface for an 8% coating. The fabric's thickness and mass per unit area were examined to check for physical changes. Aerogel coating resulted in a 4–6% increase in fabric thickness and a 6–9% increase in fabric weight. The barrier of heat and moisture transport rises with thickness. When two fabrics are of the same thickness, previous research has shown that the lower-density cloth provides better thermal insulation [150]. Coating resulted in a progressive increase in insulation in our situation, as indicated in Table 3.

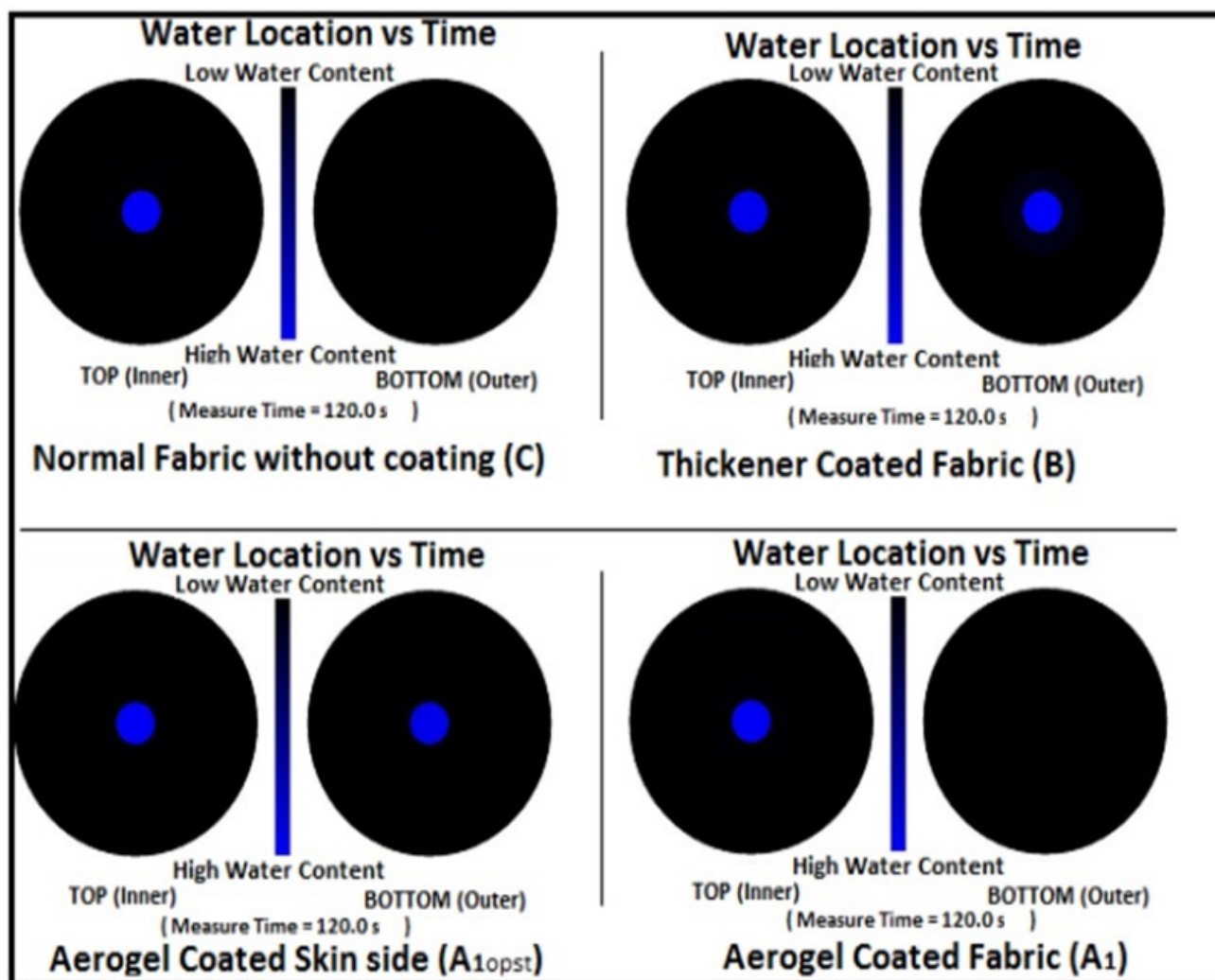


Figure 22. Maximum wetted radius lie at both top, and bottom surface. Open access, Reproduced from [144].

Table 3. Aerogel fabrics parameters. Open access, [144].

Fabric Construction	Surfaces Wetting Time (s)		Absorption (%/s)		Fabric OMMC
	Top, WT_1	Bottom, WT_b	Top, MAR_1	Bottom, MAR_b	
Aerogel Coated (A1)	5.88	119.95	58.66	0	−478.4
Thickener coated (B)	7.08	57.64	350.66	29.12	−118.5
Plain fabric (C)	6.28	119.95	332.73	0	−391.1
Aerogel skin	7.16	84.44	380.75	4.15	−393.4
Airlock (D)	7.19	119.95	363.39	0	−427.7

17. Aerogel Finishes and Coatings

To prevent air pollution from ultrafine particles, hydrophobic silica aerogel rather than its powder form is employed for aerogel superhydrophobic coatings. It is used to modify materials' surfaces so they are extremely hydrophobic while still being able to endure physical abrasion, something a regular aerogel cannot. The hydrophobic gel was combined with DOW CORNING® 2405 resin as a binder and different amounts of DOWSILTM Z-6137 silane and tetraethyl orthosilicate (TEOS) to create the superhydrophobic silica aerogel coating. Static contact angles (CA) and abrasion testing were used to describe the coating. Investigated were scanning electron micrographs of various coating formulations. According to the results, the hydrophobic gels combined with resin and Z-6137 silane have a contact angle of >179 degrees. Glass, fiber, polymers, and other materials can be coated with superhydrophobic silica aerogel [151,152].

Aerogel composites fabricated with epoxy with carbon fiber as a substrate and dip coating were utilized for the one-hour and one-and-a-half-hour marks of the epoxy cure. It was then compared with an undoped epoxy coating; there was a remarkable difference in heat conductivity values of 39% and 47%, respectively. Further proof that the aerogel particles contained nanopores came from the reflectance spectra of the coatings. Finite element techniques evaluated the aerogel coating using material parameters. The performance of the coating under cyclic thermal stresses was then predicted using the model, which was first validated using experimental data. Additionally, top and bottom coatings on a single surface were modeled and compared to the double coating system. It was discovered that the double coating system had the lowest rate of temperature change and fluctuations at steady-state, in contrast to the bottom coating, which displayed the fastest temperature drop and the highest fluctuations at steady-state conditions. The top coating's performance was average [153].

18. Aerogels Photocatalysis Applications

Photocatalysis typically involves a photocatalyst material that absorbs light and generates electron-hole pairs, which can initiate various chemical reactions. Aerogels can serve as an excellent support material for photocatalysts due to their porous nature and large surface area, allowing for high photocatalyst loading and efficient utilization of light. Aerogels can be used as a three-dimensional support matrix for anchoring photocatalytic nanoparticles (Figure 23). The high porosity of aerogels enables the dispersion of nanoparticles, providing a large active surface area for photocatalytic reactions. The highly porous structure of aerogels can trap and scatter light, increasing light-matter interactions within the photocatalyst (Figure 23). This enhances the absorption of light and promotes efficient utilization of the energy for photocatalytic reactions. Aerogels can act as protective coatings for photocatalysts, preventing their degradation and enhancing their stability. The porous structure of aerogels can also prevent the agglomeration of photocatalytic nanoparticles, maintaining their high surface area and activity. Combining aerogels with photocatalytic materials can lead to synergistic effects. For example, incorporating metal nanoparticles into aerogel structures can enhance photocatalytic activity by promoting charge separation and facilitating electron transfer processes. The choice of aerogel material depends on factors such as the desired photocatalyst, target reactions, and environmental conditions. Overall, aerogels offer promising opportunities for improving the efficiency and performance of photocatalytic systems. However, it's worth noting that the field of aerogels in photocatalysis is still evolving, and further research is needed to optimize the design and synthesis of aerogels for specific photocatalytic applications [107].

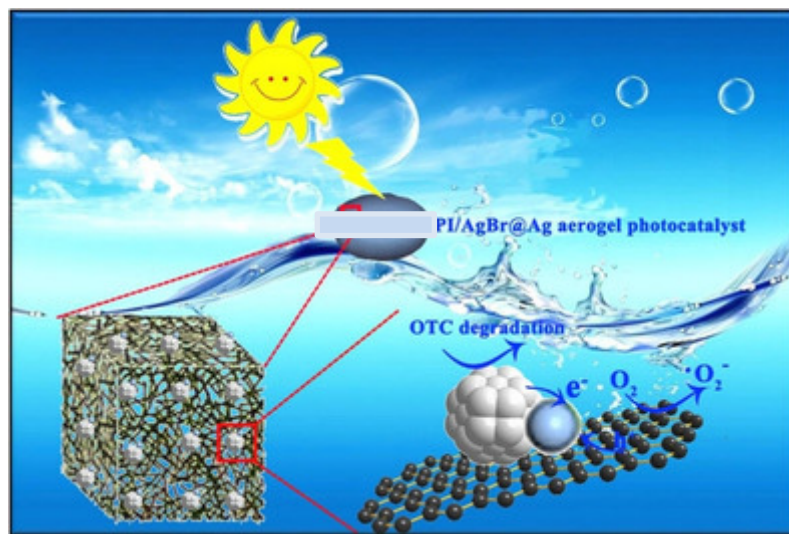


Figure 23. Aerogels applications in photocatalysis.

19. Aerogels Technical Applications

Aerogel has the most diverse applications in all technical and functional applications because of its unique physical and chemical properties (Figure 24). In the beginning, aerogel was discovered as spacesuit fabrication material for NASA projects. It can bear extreme temperatures and weather parameters and show a wispy appearance [153,154].

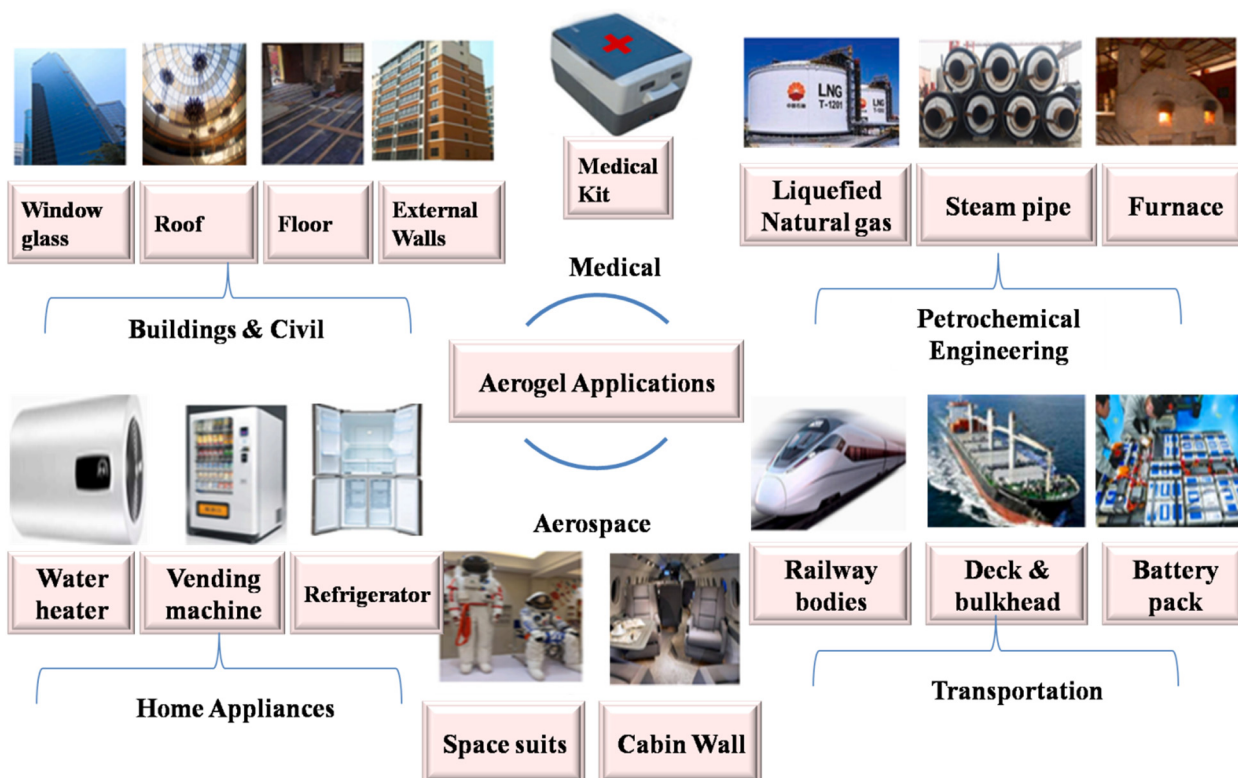


Figure 24. Aerogels applications.

In the early 21st century, aerogel started being used in astronaut applications by the ‘Stardust’ mission, with the motivation of extracting the back particles from beyond the moon. Basically, before this, dust was collected from the comet ‘Wild 2’. Aerogel was the first material to capture physical particles of dust without physically reacting with them. Basically, when the dust particle hits aerogel, its velocity speeds up to 6 times as compared

to a rifle bullet and removes it from the surface without reacting [3,155,156]. The dust particle loses its momentum when interacts with the aerogel due to the formation of more porous regions. So, it also plays a vital role in the cleaning of astronaut's parts and enhances its life. As aerogel provides insulation in advanced engineering fabrications it is utilized for space suits where insulation and flexibility are demanded [157]. Aerogel can be molded into different forms and shapes so it can be utilized as shape memory material. Carbon Aerogel materials are preferred for energy storage devices due to the networking structure of carbon atoms in them. In supercapacitors, electrode lining is made by aerogel because of its textural and unique chemical properties. Electrode lining should be porous for better transportation so aerogel porous structure is very much feasible for this [158,159]. Due to its porosity, it is also applicable in rechargeable batteries and catalyst support systems. As the graphene aerogel structure provides the highest porosity and charge mobility it was very attractive to the batteries market. In 2009, graphene aerogel anode materials were first used in battery support systems. It was further decided that graphene-based nano-porous aerogel was the best material for low-cost and high-performance energy applications. For electric vehicle electrode structures, graphene aerogel with doped cations was the best-optimized material to reduce the dependency on conventional fuel usage and to enhance aerogel market growth in the future [160].

There is an innovative and emerging application of aerogel used through the 1980s in laser fusion experiments. For the laser fusion experiment, the material should be homogenous, low dense, and pure and present in the near-spherical shells. For this, the average pore size should be smaller than 1 mm so that it must keep the liquid fuel and ensure its homogeneity [161]. Other material characteristics for this are hydrophilic in liquid deuterium–tritium, highly stable, and should be able to bear mechanical stresses and coating processes. Silica Aerogels are used for laser target materials and machined from monolithic pieces. Materials used for this are boron, silica, carbon, and organic based. Scientists are highly focused on the development of microsphere surfaces for aerogel fiber extrusions. Microporous polymeric thin doped nanomaterials are also used for this purpose [162,163]. Aerogels are widely used in hydrogen and energy applications because of their high surface area [164]. There is a very exciting application in energy loss using radiography application using Cherenkov radiation. In this setup, a monoenergetic charge particle was the source material to illuminate the imaging object. When the particle interacts with the object, it reduces its velocity and causes energy losses. The emitted photons are quite linear and it will measure the uniform velocity and density of the object. Image is the formed on the screen. It is very high speed and based on X-ray technique. Both electrons and proton beams can be utilized to form the image and it is quite economical application [165].

In aerocapacitor applications, aerogels are widely used due to their higher conductivity rate and large surface area. It provides a double layer for charge separation and a porous sheet for charge mobility. It also possesses high energy density and high power conversion as compared to traditional aerocapacitors. Electrode material provides continual charge production and high surface per unit volume due to that stored energy released with the highest power densities, e.g., 7.5 kW. Carbide-derived carbon aerogels and nitrogen-doped carbon aerogels are the best materials for this application [166]. Aerogel materials are very attractive for energetic applications. A tremendous amount of energy can be stored on its surface because of the highest porosity and low refractive index. There is much variety of its products i.e., aerogel hybrid composites, direct conversion of aerogels from energetic molecules and compound aerogels containing both reducer and oxidizer together. Lithium-ion-doped silica nanocomposite aerogel and single-metal organic framework aerogels are its most applicable products [167]. Aerogels have been used for optical applications since the 1900s because of high-temperature processes. Lanthanide-doped aerogels were considered the best material for lasing applications. Silica aerogel was not favorable for optical transmission applications. Doping of silica with radioactive phosphor and tritium converts it into the more efficient radioluminescent light source. Translucent Aerogels are

very active photocatalytic materials for solar cell applications. Solar cell applications require less dense material and with higher conductivity rate and photon absorption ability. Ni/C Aerogels have the highest conductivity among all other members so highly selective for this purpose [120]. All the aerogel varieties are recognized best insulating material for industrial and home-tech applications. It possesses high damping rates, low thermal conductivity, and low density suitable for acoustic applications. Acoustic impedance and high absorption are also characteristics. Aerogels have also been projected as a shock-absorbing material in industrial applications [168].

19.1. Thermal Insulator Applications

Energy conversion is decreased by thermal insulation. For regulation of indoor climate and to maintain proper thermal heat management, aerogel products are highly preferred for build-tech applications. Very lightweight materials (1-person structural panel) having higher fire protection class are used for rooftop materials construction. There is no colonization of fungi at the top surface of aerogel thereby enhancing its life [169]. These are also very low-cost materials. Mostly silica aerogel is utilized for domestic and industrial insulation due to its easy process but iron oxide, carbon, and organic polymer aerogel can also be used for these applications. It is also named 'frozen smoke' because its structure utilizes 99.8% of the amorphous region nothing but air [170]. Aerogel materials also lead to many applications like rooftop insulation, windows insulation, cold storage applications, and piping insulation. Silica-based aerogels, polyaniline/pectin aerogels, and Hydroxyethyl aerogels are among the best support materials for aerogel applications in the field of insulation. Carbon-silica composite Aerogels provide the best insulation with long-term durability, surface modification, and functional properties [171].

Aerogel materials with improved insulating properties have been utilized for fire retardant applications, flexible blankets, and high-performance fabrics. Aerogel-treated non-woven flexible fabrics show better thermal performance for eco-friendly garments. The "pyrogel" insulation was developed by Aspen Aerogel Inc. to be used as an effective thermal barrier in extreme weather for hikers and climbers on high peaks, where their light weight and flexibility are extremely useful [24]. Flame retardant fabrics hinder/stop the growth of flame onto the fabrics. To achieve this, aerogel coating is applied on the surface of fabric for protective clothing. Silica aerogel reduces the thermal conductivity by evacuation. As silica-biopolymers are highly hydrophobic in nature, these materials can be used to build the anti-wetting, flame-retardant surface on the textile. Silica structure can be converted into hydrophobic form by silane agents [172–174].

Green buildings, households, industrial applications, and aerogel fibers/composite structures have been explored to overcome energy consumption. To prevent heat losses and to harvest more and more solar energy, a layer of aerogel composites is embedded into two layers of PTFE that can boost insulation value (R) to 12. Aerogel blankets reduce the energy consumption rate from cooling and heating the fabric by 30–70%. It has large-scale applications in water parks, sports stadiums, and green shopping centers on the industrial scale. These also have been utilized for thermal awnings and window replacements with new energy codes. Researchers were focused on developing the insulative blanket [31]. It is produced by inserting aerogels interstitially within a fiber matrix. Matrix played an important role in enhancing the thermal properties of the final product. Aerogel composites reinforced with double-layer low-density fibers are very much suitable for thermal resistance [175]. It was comprised of two phases. Matrix was composed of low-density aerogel whereas reinforcing phase is sandwiched in between. The reinforcing is basically composed of low-density fibers, low thickness and a lesser aspect ratio. A preferred combination of composed fibrous system is an aerogel matrix bounded by short, high-aspect microfibers in which one fibrous material is continuous batting and the other one is dispersed throughout an Aerogel matrix [176].

19.2. Innovative and Medical Textile Applications

Aerogel materials also have the potential to be used for active smart textile materials and performance clothing. Piezoelectric materials based on alumina-silica are widely used for energy harvesting carpets and convert the stresses into suitable energy forms, stresses mainly come from the people walking onto it [102]. It is also used for military helmets for thermal insulation and to utilize wind and thermal energy in suitable form. Wall coverings and curtains are also mainly comprised of these aerogel structures for indoor applications. Aerogel-based smart garments are also composed of silica to map the body areas body such as the spine, kidneys, and torso. If we lead aerogel structure towards brittleness and fragility, its applications will be opened up from clothing to heatproofing and smart textiles [177]. To enhance antibacterial activity in the textile, aerogel materials are very attractive to be utilized. As the aerogel structure is porous, it hinders the growth of bacteria hence utilized for antibacterial properties. TiO_2 , ZnO aerogels solution gives higher antibacterial activity and remains active many times also showing durability. Composite aerogels having titania and zinc oxide combination show enhanced antibacterial characteristics due to incubation of bacterial zone. Aerogel solution processed with Nylon and polypropylene shows enhanced antibacterial activity. The main antibacterial property is basically due to the inherent raw material used [149,178]. For medical textiles, silica hybrid biopolymers are used for membranes and coatings. Biocompatible materials, bone substituent, and cardio-joints are fabricated by hybrid materials. Collagen, chitosan, and gelatin proteins are obtained by silica sol mixture with proteins, these sols are further processed to make biocomposite layers and hence biomaterials are fabricated. These biomaterials are highly dense, biodegradable, and have multifunctional properties. Joints are mainly fabricated by these strategies having enhanced medical applications where high strength and flexibility are the key requirements [179,180].

19.3. Aerogels in Environmental Applications

Aerogels are primarily composed of a porous network of solid materials, typically derived from silica, metal oxides, polymers, or carbon-based materials. The excellent properties make aerogels suitable for a wide range of environmental applications, thanks to their ability to address various challenges related to energy efficiency, pollution control, and sustainability [181]. Aerogels have shown promise in addressing oil spills. Their high surface area and porous structure enable them to absorb and capture oil, making them useful for cleaning up oil spills in water bodies. The absorbed oil can potentially be recovered and reused. Aerogels can be tailored to have specific pore sizes and surface chemistries, allowing them to selectively adsorb and remove contaminants from water, such as heavy metals, organic pollutants, and even microplastics. This makes them valuable for water purification and treatment [182]. Aerogels can be functionalized with chemical groups that have an affinity for capturing carbon dioxide (CO_2) from the atmosphere. These modified aerogels can potentially play a role in carbon capture and sequestration technologies to mitigate climate change. The large surface area and porous nature of aerogels also make them excellent catalyst supports. They can enhance catalytic reactions by providing a high surface area for active sites, leading to improved efficiency in various industrial processes, such as chemical production and emissions control [183]. Aerogels have been explored as materials for energy storage applications, including supercapacitors and batteries. Aerogels can be incorporated into solar panels and solar absorbers to improve their energy capture and conversion efficiency. They can also be used to create transparent insulating materials for windows that allow light in while minimizing heat transfer.

20. Future Works and Conclusions

Research is likely to focus on refining the manufacturing processes of aerogels to make them more cost-effective, scalable, and environmentally friendly. This could involve innovations in supercritical drying methods, precursor materials, and gelation techniques. One of the challenges with aerogels is their brittleness and low mechanical strength. Future

research may focus on enhancing their mechanical properties by incorporating reinforcing fibers and nanoparticles or by structurally modifying the aerogel's network. Currently, most aerogels are made from silica-based precursors. In the future, researchers might develop new types of aerogels using different precursor materials, such as polymers, metal oxides, and organic compounds. This could lead to aerogels with tailored properties for specific applications. After decades of development, a wide range of aerogel materials have been in the interest of scientists to achieve superior mechanical and thermal performance. Up to now, aerogels are still a research dimension for scientists to meet the desired thermal insulation, photocatalytic, and performance needs. Composition optimization of used raw materials, and designing novel assembly structures and hybrid structures will give a new dimension to aerogels having superior characteristics [27]. Tailoring the microstructure and composition of aerogels, and fabrication simulation of aerogels will meet the target application requirements. These scientific inquiries prompt us to investigate the underlying processes of each necessary mechanical and physicochemical property and consider the techniques of implementation in order to comprehend how to improve and combine the necessary features in a single material. Furthermore, due to preparation technological limitations, the development of aerogel products with a substantial and full structure may take years or even decades. Generally speaking, the goal of future research is to create Aerogels that are more cost-effective, perform better, and have more features.

The most persuasive and successful tactics for improving the photocatalytic and thermal insulating capabilities of aerogels, as well as promoting functionalization and industrialization, are composition optimization and microstructure reconstruction. In recent years, a wide range of aerogels with different compositions and multi-component microstructures have been developed for designers and practical life applications. The aerogel field will continue to grow at a rapid rate in the coming years, with effective raw material composition and tuned hybrid structures being key factors. With significant collaboration between academic and industrial partners, aerogels with enhanced efficiencies and tuned properties can be developed more quickly.

Author Contributions: Conceptualization, Z.A., M.A. and A.J.; methodology, Z.A., K.H.L. and A.D.; software, A.D. and M.A.; validation, M.A., Q.A.A. and M.N.; formal analysis, Z.A., M.A. and Q.A.A.; investigation, A.B., E.-J.L. and M.N. resources, K.H.L., A.J. and M.A.; writing—original Z.A. draft preparation, Z.A. and A.B.; writing—review and editing, M.A. and U.Z.; supervision, M.A.; project administration, K.H.L.; funding acquisition, K.H.L. and M.A. All authors have read and agreed to the published version of the manuscript.

Funding: This research received no external funding.

Acknowledgments: The Authors extend their appreciation to the Deanship of Scientific Research at King Khalid University for funding this research through a large group Research project under grant number RGP.2/158/44. This work was supported by the Korea Environment Industry and Technology Institute (KEITI) through the Environmental R&D Project on the Disaster Prevention of Environmental Facilities Project, funded by the Korea Ministry of Environment (MOE) (2020002870004).

Conflicts of Interest: The authors declare no conflict of interest. We declare that we have no commercial or associative interest in the work submitted that would create a conflict of interest.

References

1. Guo, J.; Fu, S.; Deng, Y.; Xu, X.; Laima, S.; Liu, D.; Zhang, P.; Zhou, J.; Zhao, H.; Yu, H. Hypocrystalline ceramic aerogels for thermal insulation at extreme conditions. *Nature* **2022**, *606*, 909–916. [[CrossRef](#)]
2. Ganesamoorthy, R.; Vadivel, V.K.; Kumar, R.; Kushwaha, O.S.; Mamane, H. Aerogels for water treatment: A review. *J. Clean. Prod.* **2021**, *329*, 129713. [[CrossRef](#)]
3. Jones, S.M. Aerogel: Space exploration applications. *J. Sol-Gel Sci. Technol.* **2006**, *40*, 351–357. [[CrossRef](#)]
4. Chen, Y.; Zhang, L.; Yang, Y.; Pang, B.; Xu, W.; Duan, G.; Jiang, S.; Zhang, K. Recent progress on nanocellulose aerogels: Preparation, modification, composite fabrication, applications. *Adv. Mater.* **2021**, *33*, 2005569. [[CrossRef](#)]
5. Ghalekhondabi, I.; Ardjmand, E.; Weckman, G.R.; Young, W.A. An overview of energy demand forecasting methods published in 2005–2015. *Energy Syst.* **2017**, *8*, 411–447. [[CrossRef](#)]

6. Sorrell, S. Reducing energy demand: A review of issues, challenges and approaches. *Renew. Sustain. Energy Rev.* **2015**, *47*, 74–82. [[CrossRef](#)]
7. Van Ruijven, B.J.; De Cian, E.; Sue Wing, I. Amplification of future energy demand growth due to climate change. *Nat. Commun.* **2019**, *10*, 2762. [[CrossRef](#)]
8. Bertoldi, P. Overview of the European Union policies to promote more sustainable behaviours in energy end-users. In *Energy and Behaviour*; Elsevier: Amsterdam, The Netherlands, 2020; pp. 451–477.
9. Economidou, M.; Todeschi, V.; Bertoldi, P.; D'Agostino, D.; Zangheri, P.; Castellazzi, L. Review of 50 years of EU energy efficiency policies for buildings. *Energy Build.* **2020**, *225*, 110322. [[CrossRef](#)]
10. Lucarelli, C.; Mazzoli, C.; Rancan, M.; Severini, S. Classification of sustainable activities: EU taxonomy and scientific literature. *Sustainability* **2020**, *12*, 6460. [[CrossRef](#)]
11. Jelle, B.P. Traditional, state-of-the-art and future thermal building insulation materials and solutions—Properties, requirements and possibilities. *Energy Build.* **2011**, *43*, 2549–2563. [[CrossRef](#)]
12. Feng, J.; Su, B.-L.; Xia, H.; Zhao, S.; Gao, C.; Wang, L.; Ogbeide, O.; Feng, J.; Hasan, T. Printed aerogels: Chemistry, processing, and applications. *Chem. Soc. Rev.* **2021**, *50*, 3842–3888. [[CrossRef](#)] [[PubMed](#)]
13. Sen, S.; Singh, A.; Bera, C.; Roy, S.; Kailasam, K. Recent developments in biomass derived cellulose aerogel materials for thermal insulation application: A review. *Cellulose* **2022**, *29*, 4805–4833. [[CrossRef](#)]
14. Li, C.; Chen, Z.; Dong, W.; Lin, L.; Zhu, X.; Liu, Q.; Zhang, Y.; Zhai, N.; Zhou, Z.; Wang, Y. A review of silicon-based aerogel thermal insulation materials: Performance optimization through composition and microstructure. *J. Non-Cryst. Solids* **2021**, *553*, 120517. [[CrossRef](#)]
15. Du, A.; Zhou, B.; Zhang, Z.; Shen, J. A special material or a new state of matter: A review and reconsideration of the aerogel. *Materials* **2013**, *6*, 941–968. [[CrossRef](#)] [[PubMed](#)]
16. Liu, Q.; Yan, K.; Chen, J.; Xia, M.; Li, M.; Liu, K.; Wang, D.; Wu, C.; Xie, Y. Recent advances in novel aerogels through the hybrid aggregation of inorganic nanomaterials and polymeric fibers for thermal insulation. *Aggregate* **2021**, *2*, e30. [[CrossRef](#)]
17. Wang, L.; Xu, H.; Gao, J.; Yao, J.; Zhang, Q. Recent progress in metal-organic frameworks-based hydrogels and aerogels and their applications. *Coord. Chem. Rev.* **2019**, *398*, 213016. [[CrossRef](#)]
18. Schaefer, D.W.; Keefer, K.D. Structure of random porous materials: Silica aerogel. *Phys. Rev. Lett.* **1986**, *56*, 2199. [[CrossRef](#)]
19. Worsley, M.A.; Pauzauskie, P.J.; Olson, T.Y.; Biener, J.; Satcher, J.H., Jr.; Baumann, T.F. Synthesis of graphene aerogel with high electrical conductivity. *J. Am. Chem. Soc.* **2010**, *132*, 14067–14069. [[CrossRef](#)]
20. An, L.; Wang, J.; Petit, D.; Armstrong, J.N.; Hanson, K.; Hamilton, J.; Souza, M.; Zhao, D.; Li, C.; Liu, Y. An all-ceramic, anisotropic, and flexible aerogel insulation material. *Nano Lett.* **2020**, *20*, 3828–3835. [[CrossRef](#)]
21. Wittwer, V. Development of aerogel windows. *J. Non-Cryst. Solids* **1992**, *145*, 233–236. [[CrossRef](#)]
22. Baktash, A.; Amiri, O.; Sasani, A. Improve efficiency of perovskite solar cells by using magnesium doped ZnO and TiO₂ compact layers. *Superlattices Microstruct.* **2016**, *93*, 128–137. [[CrossRef](#)]
23. Joly, M.; Bourdoukan, P.; Ibrahim, M.; Stipetic, M.; Dantz, S.; Nocentini, K.; Aulagnier, M.; Caiazza, F.G.; Fiorentino, B. Competitive high performance Aerogel-Based Composite material for the European insulation market. *Energy Procedia* **2017**, *122*, 859–864. [[CrossRef](#)]
24. Berardi, U. Aerogel-enhanced insulation for building applications. In *Nanotechnology in Eco-Efficient Construction*; Elsevier: Amsterdam, The Netherlands, 2019; pp. 395–416.
25. Herrmann, G.; Iden, R.; Mielke, M.; Teich, F.; Ziegler, B. On the way to commercial production of silica aerogel. *J. Non-Cryst. Solids* **1995**, *186*, 380–387. [[CrossRef](#)]
26. Rahmanian, V.; Pirzada, T.; Wang, S.; Khan, S.A. Cellulose-Based Hybrid Aerogels: Strategies toward Design and Functionality. *Adv. Mater.* **2021**, *33*, 2102892. [[CrossRef](#)] [[PubMed](#)]
27. An, L.; Wang, J.; Petit, D.; Armstrong, J.N.; Li, C.; Hu, Y.; Huang, Y.; Shao, Z.; Ren, S. A scalable crosslinked fiberglass-aerogel thermal insulation composite. *Appl. Mater. Today* **2020**, *21*, 100843. [[CrossRef](#)]
28. Arshad, Z.; Khoja, A.H.; Shakir, S.; Afzal, A.; Mujtaba, M.A.; Soudagar, M.E.M.; Fayaz, H.; Saleel, C. A.; Farukh, S.; Saeed, M. Magnesium doped TiO₂ as an efficient electron transport layer in perovskite solar cells. *Case Stud. Therm. Eng.* **2021**, *26*, 101101. [[CrossRef](#)]
29. Zhao, S.; Siqueira, G.; Drdova, S.; Norris, D.; Ubert, C.; Bonnin, A.; Galmarini, S.; Ganobjak, M.; Pan, Z.; Brunner, S. Additive manufacturing of silica aerogels. *Nature* **2020**, *584*, 387–392. [[CrossRef](#)]
30. Koebel, M.; Rigacci, A.; Achard, P. Aerogel-based thermal superinsulation: An overview. *J. Sol-Gel Sci. Technol.* **2012**, *63*, 315–339. [[CrossRef](#)]
31. Mazrouei-Sebdani, Z.; Begum, H.; Schoenwald, S.; Horoshenkov, K.V.; Malfait, W.J. A review on silica aerogel-based materials for acoustic applications. *J. Non-Cryst. Solids* **2021**, *562*, 120770. [[CrossRef](#)]
32. Maleki, H.; Durães, L.; Portugal, A. An overview on silica aerogels synthesis and different mechanical reinforcing strategies. *J. Non-Cryst. Solids* **2014**, *385*, 55–74. [[CrossRef](#)]
33. Sehaqui, H.; Zhou, Q.; Berglund, L.A. High-porosity aerogels of high specific surface area prepared from nanofibrillated cellulose (NFC). *Compos. Sci. Technol.* **2011**, *71*, 1593–1599. [[CrossRef](#)]
34. Gesser, H.; Goswami, P. Aerogels and related porous materials. *Chem. Rev.* **1989**, *89*, 765–788. [[CrossRef](#)]

35. Zheng, Q.; Fang, L.; Guo, H.; Yang, K.; Cai, Z.; Meador, M.A.B.; Gong, S. Highly porous polymer aerogel film-based triboelectric nanogenerators. *Adv. Funct. Mater.* **2018**, *28*, 1706365. [[CrossRef](#)]
36. Dorcheh, A.S.; Abbasi, M. Silica aerogel; synthesis, properties and characterization. *J. Mater. Process. Technol.* **2008**, *199*, 10–26. [[CrossRef](#)]
37. Dai, H.; Jun, Z.; Yin, Y.; Shao, G.; Yu, C. Synthesis of Ag doped SiO₂-TiO₂ aerogels with nano-sized microcrystalline anatase structure through IL control. *IOP Conf. Ser. Shangai, China.: Mater. Sci. Eng.* **2019**, *587*, 012016. [[CrossRef](#)]
38. Koyuncu, D.D.E.; Okur, M. Investigation of dye removal ability and reusability of green and sustainable silica and carbon-silica hybrid aerogels prepared from paddy waste ash. *Colloids Surf. A Physicochem. Eng. Asp.* **2021**, *628*, 127370. [[CrossRef](#)]
39. Wan, W.; Zhang, R.; Ma, M.; Zhou, Y. Monolithic aerogel photocatalysts: A review. *J. Mater. Chem. A* **2018**, *6*, 754–775. [[CrossRef](#)]
40. Wong, K.J.; Foo, J.J.; Siang, T.J.; Ong, W.J. Shining Light on Carbon Aerogel Photocatalysts: Unlocking the Potentials in the Quest for Revolutionizing Solar-to-Chemical Conversion and Environmental Remediation. *Adv. Funct. Mater.* **2023**, 2306014. [[CrossRef](#)]
41. Schreck, M.; Kleger, N.; Matter, F.; Kwon, J.; Tervoort, E.; Masania, K.; Studart, A.R.; Niederberger, M. 3D Printed Scaffolds for Monolithic Aerogel Photocatalysts with Complex Geometries. *Small* **2021**, *17*, 2104089. [[CrossRef](#)]
42. Ge, B.; Ren, G.; Yang, H.; Yang, J.; Pu, X.; Li, W.; Jin, C.; Zhang, Z. Fabrication of BiOBr-silicone aerogel photocatalyst in an aqueous system with degradation performance by sol-gel method. *Sci. China Technol. Sci.* **2020**, *63*, 859–865. [[CrossRef](#)]
43. Ferreira-Neto, E.P.; Worsley, M.A.; Rodrigues-Filho, U.P. Towards thermally stable aerogel photocatalysts: TiCl₄-based sol-gel routes for the design of nanostructured silica-titania aerogel with high photocatalytic activity and outstanding thermal stability. *J. Environ. Chem. Eng.* **2019**, *7*, 103425. [[CrossRef](#)]
44. Hasanpour, M.; Hatami, M. Photocatalytic performance of aerogels for organic dyes removal from wastewaters: Review study. *J. Mol. Liquids* **2020**, *309*, 113094. [[CrossRef](#)]
45. Zhao, X.; Yi, X.; Wang, X.; Chu, W.; Guo, S.; Zhang, J.; Liu, B.; Liu, X. Constructing efficient polyimide (PI)/Ag aerogel photocatalyst by ethanol supercritical drying technique for hydrogen evolution. *Appl. Surf. Sci.* **2020**, *502*, 144187. [[CrossRef](#)]
46. Sleator, T.; Bernasconi, A.; Posselt, D.; Kjems, J.; Ott, H. Low-temperature specific heat and thermal conductivity of silica aerogels. *Phys. Rev. Lett.* **1991**, *66*, 1070. [[CrossRef](#)] [[PubMed](#)]
47. Yanagi, R.; Takemoto, R.; Ono, K.; Ueno, T. Light-induced levitation of ultralight carbon aerogels via temperature control. *Sci. Rep.* **2021**, *11*, 12413. [[CrossRef](#)]
48. Scheuerpflug, P.; Hauck, M.; Fricke, J. Thermal properties of silica aerogels between 1.4 and 330 K. *J. Non-Cryst. Solids* **1992**, *145*, 196–201. [[CrossRef](#)]
49. Ebert, H.-P. Thermal properties of aerogels. In *Aerogels Handbook*; Springer: Berlin/Heidelberg, Germany, 2011; pp. 537–564.
50. Bernasconi, A.; Sleator, T.; Posselt, D.; Ott, H. Dynamic technique for measurement of the thermal conductivity and the specific heat: Application to silica aerogels. *Rev. Sci. Instrum.* **1990**, *61*, 2420–2426. [[CrossRef](#)]
51. Wiener, M.; Reichenauer, G.; Braxmeier, S.; Hemberger, F.; Ebert, H.-P. Carbon aerogel-based high-temperature thermal insulation. *Int. J. Thermophys.* **2009**, *30*, 1372–1385. [[CrossRef](#)]
52. Strzałkowski, J.; Garbalińska, H. Thermal and strength properties of lightweight concretes with the addition of aerogel particles. *Adv. Cem. Res.* **2016**, *28*, 567–575. [[CrossRef](#)]
53. Li, D.; Zhang, C.; Li, Q.; Liu, C.; Arici, M.; Wu, Y. Thermal performance evaluation of glass window combining silica aerogels and phase change materials for cold climate of China. *Appl. Therm. Eng.* **2020**, *165*, 114547. [[CrossRef](#)]
54. Bellini, T.; Clark, N.A.; Muzny, C.D.; Wu, L.; Garland, C.W.; Schaefer, D.W.; Oliver, B.J. Phase behavior of the liquid crystal 8CB in a silica aerogel. *Phys. Rev. Lett.* **1992**, *69*, 788. [[CrossRef](#)] [[PubMed](#)]
55. Zeng, S.; Hunt, A.; Greif, R. Theoretical modeling of carbon content to minimize heat transfer in silica aerogel. *J. Non-Cryst. Solids* **1995**, *186*, 271–277. [[CrossRef](#)]
56. Hasan, M.A.; Sangashetty, R.; Esther, A.C.M.; Patil, S.B.; Sherikar, B.N.; Dey, A. Prospect of thermal insulation by silica aerogel: A brief review. *J. Inst. Eng. (India) Ser. D* **2017**, *98*, 297–304. [[CrossRef](#)]
57. Du, A.; Wang, H.; Zhou, B.; Zhang, C.; Wu, X.; Ge, Y.; Niu, T.; Ji, X.; Zhang, T.; Zhang, Z. Multifunctional silica nanotube aerogels inspired by polar bear hair for light management and thermal insulation. *Chem. Mater.* **2018**, *30*, 6849–6857. [[CrossRef](#)]
58. Wang, F.; Dou, L.; Dai, J.; Li, Y.; Huang, L.; Si, Y.; Yu, J.; Ding, B. In situ synthesis of biomimetic silica nanofibrous aerogels with temperature-invariant superelasticity over one million compressions. *Angew. Chem.* **2020**, *132*, 8362–8369. [[CrossRef](#)]
59. Wilson, S.M.; Gabriel, V.A.; Tezel, F.H. Adsorption of components from air on silica aerogels. *Microporous Mesoporous Mater.* **2020**, *305*, 110297. [[CrossRef](#)]
60. Tian, X.; Liu, J.; Wang, Y.; Shi, F.; Shan, Z.; Zhou, J.; Liu, J. Adsorption of antibiotics from aqueous solution by different aerogels. *J. Non-Cryst. Solids* **2019**, *505*, 72–78. [[CrossRef](#)]
61. Cheng, H.; Fan, Z.; Hong, C.; Zhang, X. Lightweight multiscale hybrid carbon-quartz fiber fabric reinforced phenolic-silica aerogel nanocomposite for high temperature thermal protection. *Compos. Part A Appl. Sci. Manuf.* **2021**, *143*, 106313. [[CrossRef](#)]
62. Xie, T.; He, Y.-L. Heat transfer characteristics of silica aerogel composite materials: Structure reconstruction and numerical modeling. *Int. J. Heat Mass Transf.* **2016**, *95*, 621–635. [[CrossRef](#)]
63. Wei, G.; Liu, Y.; Zhang, X.; Du, X. Radiative heat transfer study on silica aerogel and its composite insulation materials. *J. Non-Cryst. Solids* **2013**, *362*, 231–236. [[CrossRef](#)]
64. Yokogawa, H.; Yokoyama, M. Hydrophobic silica aerogels. *J. Non-Cryst. Solids* **1995**, *186*, 23–29. [[CrossRef](#)]

65. Korhonen, J.T.; Kettunen, M.; Ras, R.H.; Ikkala, O. Hydrophobic nanocellulose aerogels as floating, sustainable, reusable, and recyclable oil absorbents. *ACS Appl. Mater. Interfaces* **2011**, *3*, 1813–1816. [[CrossRef](#)] [[PubMed](#)]
66. He, S.; Huang, Y.; Chen, G.; Feng, M.; Dai, H.; Yuan, B.; Chen, X. Effect of heat treatment on hydrophobic silica aerogel. *J. Hazard. Mater.* **2019**, *362*, 294–302. [[CrossRef](#)] [[PubMed](#)]
67. Schwertfeger, F.; Frank, D.; Schmidt, M. Hydrophobic waterglass based aerogels without solvent exchange or supercritical drying. *J. Non-Cryst. Solids* **1998**, *225*, 24–29. [[CrossRef](#)]
68. Ge, D.; Yang, L.; Li, Y.; Zhao, J. Hydrophobic and thermal insulation properties of silica aerogel/epoxy composite. *J. Non-Cryst. Solids* **2009**, *355*, 2610–2615. [[CrossRef](#)]
69. Alwin, S.; Sahaya Shajan, X. Aerogels: Promising nanostructured materials for energy conversion and storage applications. *Mater. Renew. Sustain. Energy* **2020**, *9*, 7. [[CrossRef](#)]
70. Akhter, F.; Soomro, S.A.; Inglezakis, V.J. Silica aerogels; a review of synthesis, applications and fabrication of hybrid composites. *J. Porous Mater.* **2021**, *28*, 1387–1400. [[CrossRef](#)]
71. Tabata, M.; Adachi, I.; Kawai, H.; Sumiyoshi, T.; Yokogawa, H. Hydrophobic silica aerogel production at KEK. *Nuclear Instrum. Methods Phys. Res. Sect. A Accel. Spectrom. Detect. Assoc. Equip.* **2012**, *668*, 64–70. [[CrossRef](#)]
72. Smirnova, I.; Suttiruengwong, S.; Arlt, W. Feasibility study of hydrophilic and hydrophobic silica aerogels as drug delivery systems. *J. Non-Cryst. Solids* **2004**, *350*, 54–60. [[CrossRef](#)]
73. Dai, S.; Ju, Y.; Gao, H.; Lin, J.; Pennycook, S.; Barnes, C. Preparation of silica aerogel using ionic liquids as solvents. *Chem. Commun.* **2000**, *3*, 243–244. [[CrossRef](#)]
74. Lee, K.-H.; Kim, S.-Y.; Yoo, K.-P. Low-density, hydrophobic aerogels. *J. Non-Cryst. Solids* **1995**, *186*, 18–22. [[CrossRef](#)]
75. Zeng, S.; Hunt, A.; Greif, R. Transport properties of gas in silica aerogel. *J. Non-Cryst. Solids* **1995**, *186*, 264–270. [[CrossRef](#)]
76. Shi, M.; Tang, C.; Yang, X.; Zhou, J.; Jia, F.; Han, Y.; Li, Z. Superhydrophobic silica aerogels reinforced with polyacrylonitrile fibers for adsorbing oil from water and oil mixtures. *RSC Adv.* **2017**, *7*, 4039–4045. [[CrossRef](#)]
77. Ayen, R.; Iacobucci, P. Metal oxide aerogel preparation by supercritical extraction. *Rev. Chem. Eng.* **1988**, *5*, 157–198. [[CrossRef](#)]
78. Gash, A.E.; Tillotson, T.M.; Satcher Jr, J.H.; Hrubesh, L.W.; Simpson, R.L. New sol–gel synthetic route to transition and main-group metal oxide aerogels using inorganic salt precursors. *J. Non-Cryst. Solids* **2001**, *285*, 22–28. [[CrossRef](#)]
79. Benad, A.; Jürries, F.; Vetter, B.; Klemmed, B.; Hübner, R.; Leyens, C.; Eychmüller, A. Mechanical properties of metal oxide aerogels. *Chem. Mater.* **2018**, *30*, 145–152. [[CrossRef](#)]
80. Li, J.; Wang, X.; Huang, Q.; Gamboa, S.; Sebastian, P. Studies on preparation and performances of carbon aerogel electrodes for the application of supercapacitor. *J. Power Sources* **2006**, *158*, 784–788. [[CrossRef](#)]
81. Meena, A.K.; Mishra, G.; Rai, P.; Rajagopal, C.; Nagar, P. Removal of heavy metal ions from aqueous solutions using carbon aerogel as an adsorbent. *J. Hazard. Mater.* **2005**, *122*, 161–170. [[CrossRef](#)]
82. Ying, T.-Y.; Yang, K.-L.; Yiacoumi, S.; Tsouris, C. Electrosorption of ions from aqueous solutions by nanostructured carbon aerogel. *J. Colloid Interface Sci.* **2002**, *250*, 18–27. [[CrossRef](#)]
83. Hwang, S.-W.; Hyun, S.-H. Capacitance control of carbon aerogel electrodes. *J. Non-Cryst. Solids* **2004**, *347*, 238–245. [[CrossRef](#)]
84. Hao, P.; Zhao, Z.; Tian, J.; Li, H.; Sang, Y.; Yu, G.; Cai, H.; Liu, H.; Wong, C.; Umar, A. Hierarchical porous carbon aerogel derived from bagasse for high performance supercapacitor electrode. *Nanoscale* **2014**, *6*, 12120–12129. [[CrossRef](#)]
85. Xu, P.; Drewes, J.E.; Heil, D.; Wang, G. Treatment of brackish produced water using carbon aerogel-based capacitive deionization technology. *Water Res.* **2008**, *42*, 2605–2617. [[CrossRef](#)]
86. Yang, K.-L.; Ying, T.-Y.; Yiacoumi, S.; Tsouris, C.; Vittoratos, E.S. Electrosorption of ions from aqueous solutions by carbon aerogel: An electrical double-layer model. *Langmuir* **2001**, *17*, 1961–1969. [[CrossRef](#)]
87. Zhu, C.; Han, T.Y.-J.; Duoss, E.B.; Golobic, A.M.; Kuntz, J.D.; Spadaccini, C.M.; Worsley, M.A. Highly compressible 3D periodic graphene aerogel microlattices. *Nat. Commun.* **2015**, *6*, 6962. [[CrossRef](#)]
88. Zhang, X.; Sui, Z.; Xu, B.; Yue, S.; Luo, Y.; Zhan, W.; Liu, B. Mechanically strong and highly conductive graphene aerogel and its use as electrodes for electrochemical power sources. *J. Mater. Chem.* **2011**, *21*, 6494–6497. [[CrossRef](#)]
89. Xu, Z.; Zhang, Y.; Li, P.; Gao, C. Strong, conductive, lightweight, neat graphene aerogel fibers with aligned pores. *ACS Nano* **2012**, *6*, 7103–7113. [[CrossRef](#)] [[PubMed](#)]
90. Yang, M.; Zhao, N.; Cui, Y.; Gao, W.; Zhao, Q.; Gao, C.; Bai, H.; Xie, T. Biomimetic architected graphene aerogel with exceptional strength and resilience. *ACS Nano* **2017**, *11*, 6817–6824. [[CrossRef](#)] [[PubMed](#)]
91. El Kadib, A.; Bousmina, M. Chitosan bio-based organic–inorganic hybrid aerogel microspheres. *Chem.–Eur. J.* **2012**, *18*, 8264–8277. [[CrossRef](#)] [[PubMed](#)]
92. Hu, H.; Zhao, Z.; Wan, W.; Gogotsi, Y.; Qiu, J. Polymer/graphene hybrid aerogel with high compressibility, conductivity, and “sticky” superhydrophobicity. *ACS Appl. Mater. Interfaces* **2014**, *6*, 3242–3249. [[CrossRef](#)] [[PubMed](#)]
93. Shah, N.; Lin, D. Composite Aerogels for Biomedical and Environmental Applications. *Curr. Pharm. Des.* **2020**, *26*, 5807–5818. [[CrossRef](#)]
94. Zhao, X.; Yang, F.; Wang, Z.; Ma, P.; Dong, W.; Hou, H.; Fan, W.; Liu, T. Mechanically strong and thermally insulating polyimide aerogels by homogeneity reinforcement of electrospun nanofibers. *Compos. Part B Eng.* **2020**, *182*, 107624. [[CrossRef](#)]

95. Yue, Y.; Liu, N.; Ma, Y.; Wang, S.; Liu, W.; Luo, C.; Zhang, H.; Cheng, F.; Rao, J.; Hu, X. Highly self-healable 3D microsupercapacitor with MXene–graphene composite aerogel. *ACS Nano* **2018**, *12*, 4224–4232. [[CrossRef](#)] [[PubMed](#)]
96. Anderson, M.L.; Stroud, R.M.; Morris, C.A.; Merzbacher, C.I.; Rolison, D.R. Tailoring advanced nanoscale materials through synthesis of composite aerogel architectures. *Adv. Eng. Mater.* **2000**, *2*, 481–488. [[CrossRef](#)]
97. Nawaz, M.; Miran, W.; Jang, J.; Lee, D.S. One-step hydrothermal synthesis of porous 3D reduced graphene oxide/TiO₂ aerogel for carbamazepine photodegradation in aqueous solution. *App. Catal. B Environ.* **2017**, *203*, 85–95. [[CrossRef](#)]
98. Zu, G.; Shen, J.; Wei, X.; Ni, X.; Zhang, Z.; Wang, J.; Liu, G. Preparation and characterization of monolithic alumina aerogels. *J. Non-Cryst. Solids* **2011**, *357*, 2903–2906. [[CrossRef](#)]
99. Fan, W.; Zuo, L.; Zhang, Y.; Chen, Y.; Liu, T. Mechanically strong polyimide/carbon nanotube composite aerogels with controllable porous structure. *Compos. Sci. Technol.* **2018**, *156*, 186–191. [[CrossRef](#)]
100. Guo, W.; Liu, J.; Zhang, P.; Song, L.; Wang, X.; Hu, Y. Multi-functional hydroxyapatite/polyvinyl alcohol composite aerogels with self-cleaning, superior fire resistance and low thermal conductivity. *Compos. Sci. Technol.* **2018**, *158*, 128–136. [[CrossRef](#)]
101. Bryning, M.B.; Milkie, D.E.; Islam, M.F.; Hough, L.A.; Kikkawa, J.M.; Yodh, A.G. Carbon nanotube aerogels. *Adv. Mater.* **2007**, *19*, 661–664. [[CrossRef](#)]
102. Kim, K.H.; Oh, Y.; Islam, M. Graphene coating makes carbon nanotube aerogels superelastic and resistant to fatigue. *Nat. Nanotechnol.* **2012**, *7*, 562–566. [[CrossRef](#)]
103. Merillas, B.; Villafañe, F.; Rodríguez-Pérez, M.Á. Super-insulating transparent polyisocyanurate-polyurethane aerogels: Analysis of thermal conductivity and mechanical properties. *Nanomaterials* **2022**, *12*, 2409. [[CrossRef](#)]
104. Maiuolo, L.; Olivito, F.; Algeri, V.; Costanzo, P.; Jiritano, A.; Tallarida, M.A.; Tursi, A.; Sposato, C.; Feo, A.; De Nino, A. Synthesis, characterization and mechanical properties of novel bio-based polyurethane foams using cellulose-derived polyol for chain extension and cellulose citrate as a thickener additive. *Polymers* **2021**, *13*, 2802. [[CrossRef](#)] [[PubMed](#)]
105. Maleki, H.; Hüsing, N. Current status, opportunities and challenges in catalytic and photocatalytic applications of aerogels: Environmental protection aspects. *Appl. Catal. B Environ.* **2018**, *221*, 530–555. [[CrossRef](#)]
106. Zhao, X.; Zhang, J.; Wang, X.; Zhang, J.; Liu, B.; Yi, X. Polyimide aerogels crosslinked with MWCNT for enhanced visible-light photocatalytic activity. *Appl. Surf. Sci.* **2019**, *478*, 266–274. [[CrossRef](#)]
107. Yan, S.; Song, H.; Li, Y.; Yang, J.; Jia, X.; Wang, S.; Yang, X. Integrated reduced graphene oxide/polypyrrole hybrid aerogels for simultaneous photocatalytic decontamination and water evaporation. *Appl. Catal. B Environ.* **2022**, *301*, 120820. [[CrossRef](#)]
108. Bai, Y.; Yi, X.; Li, B.; Chen, S.; Fan, Z. Constructing porous polyimide/carbon quantum dots aerogel with efficient photocatalytic property under visible light. *Appl. Surf. Sci.* **2022**, *578*, 151993. [[CrossRef](#)]
109. Zhi, M.; Tang, H.; Wu, M.; Ouyang, C.; Hong, Z.; Wu, N. Synthesis and Photocatalysis of Metal Oxide Aerogels: A Review. *Energy Fuels* **2022**, *36*, 11359–11379. [[CrossRef](#)]
110. Jiang, G.; Wang, J.; Li, N.; Hübner, R.; Georgi, M.; Cai, B.; Li, Z.; Lesnyak, V.; Gaponik, N.; Eychmüller, A. Self-supported three-dimensional quantum dot aerogels as a promising photocatalyst for CO₂ reduction. *Chem. Mater.* **2022**, *34*, 2687–2695. [[CrossRef](#)]
111. Korkmaz, S.; Kariper, İ.A. Graphene and graphene oxide based aerogels: Synthesis, characteristics and supercapacitor applications. *J. Energy Storage* **2020**, *27*, 101038. [[CrossRef](#)]
112. Liu, W.; Herrmann, A.-K.; Bigall, N.C.; Rodriguez, P.; Wen, D.; Oezaslan, M.; Schmidt, T.J.; Gaponik, N.; Eychmüller, A. Noble Metal Aerogels Synthesis, Characterization, and Application as Electrocatalysts. *Accounts Chem. Res.* **2015**, *48*, 154–162. [[CrossRef](#)]
113. Kharissova, O.V.; Ibarra Torres, C.E.; González, L.T.; Kharisov, B.I. All-carbon hybrid aerogels: Synthesis, properties, and applications. *Ind. Eng. Chem. Res.* **2019**, *58*, 16258–16286. [[CrossRef](#)]
114. Zhi, D.; Li, T.; Li, J.; Ren, H.; Meng, F. A review of three-dimensional graphene-based aerogels: Synthesis, structure and application for microwave absorption. *Compos. Part B Eng.* **2021**, *211*, 108642. [[CrossRef](#)]
115. Campbell, L.; Na, B.; Ko, E. Synthesis and characterization of titania aerogels. *Chem. Mater.* **1992**, *4*, 1329–1333. [[CrossRef](#)]
116. Rao, A.V.; Bhagat, S.D.; Hirashima, H.; Pajonk, G. Synthesis of flexible silica aerogels using methyltrimethoxysilane (MTMS) precursor. *J. Colloid Interface Sci.* **2006**, *300*, 279–285.
117. Minisy, I.M.; Acharya, U.; Veigel, S.; Morávková, Z.; Taboubi, O.; Hodan, J.; Breitenbach, S.; Unterweger, C.; Gindl-Altmutter, W.; Bober, P. Sponge-like polypyrrole–nanofibrillated cellulose aerogels: Synthesis and application. *J. Mater. Chem. C* **2021**, *9*, 12615–12623. [[CrossRef](#)]
118. Aegerter, M.A.; Leventis, N.; Koebel, M.M. *Aerogels Handbook*; Springer Science & Business Media: Berlin, Germany, 2011.
119. Maleki, H.; Durães, L.; García-González, C.A.; Del Gaudio, P.; Portugal, A.; Mahmoudi, M. Synthesis and biomedical applications of aerogels: Possibilities and challenges. *Adv. Colloid Interface Sci.* **2016**, *236*, 1–27. [[CrossRef](#)] [[PubMed](#)]
120. Ratke, L.; Gurikov, P. *The Chemistry and Physics of Aerogels: Synthesis, Processing, and Properties*; Cambridge University Press: Cambridge, UK, 2021.
121. Stolarski, M.; Walendziewski, J.; Steininger, M.; Pniak, B. Synthesis and characteristic of silica aerogels. *Appl. Catal. A Gen.* **1999**, *177*, 139–148. [[CrossRef](#)]
122. Morris, C.A.; Anderson, M.L.; Stroud, R.M.; Merzbacher, C.I.; Rolison, D.R. Silica sol as a nanogel: Flexible synthesis of composite aerogels. *Science* **1999**, *284*, 622–624. [[CrossRef](#)]

123. Esquivias, L.; Pinero, M.; Morales-Flórez, V.; de la Rosa-Fox, N. Aerogels synthesis by sonocatalysis: Sonogels. In *Aerogels Handbook*; Springer: Berlin/Heidelberg, Germany, 2011; pp. 419–445.
124. Hoepfner, S.; Ratke, L.; Milow, B. Synthesis and characterisation of nanofibrillar cellulose aerogels. *Cellulose* **2008**, *15*, 121–129. [[CrossRef](#)]
125. Pinelli, F.; Nespoli, T.; Rossi, F. Graphene Oxide-Chitosan Aerogels: Synthesis, Characterization, and Use as Adsorbent Material for Water Contaminants. *Gels* **2021**, *7*, 149. [[CrossRef](#)]
126. Jafari, S.; Dehghani, M.; Nasirizadeh, N.; Baghersad, M.H.; Azimzadeh, M. Label-free electrochemical detection of Cloxacillin antibiotic in milk samples based on molecularly imprinted polymer and graphene oxide-gold nanocomposite. *Measurement* **2019**, *145*, 22–29. [[CrossRef](#)]
127. Du, Y.; Zhang, X.; Wang, J.; Liu, Z.; Zhang, K.; Ji, X.; You, Y.; Zhang, X. Reaction-spun transparent silica aerogel fibers. *ACS Nano* **2020**, *14*, 11919–11928. [[CrossRef](#)] [[PubMed](#)]
128. Karadagli, I.; Schulz, B.; Schestakow, M.; Milow, B.; Gries, T.; Ratke, L. Production of porous cellulose aerogel fibers by an extrusion process. *J. Supercrit. Fluids* **2015**, *106*, 105–114. [[CrossRef](#)]
129. Yang, H.; Wang, Z.; Liu, Z.; Cheng, H.; Li, C. Continuous, strong, porous silk fibroin-based aerogel fibers toward textile thermal insulation. *Polymers* **2019**, *11*, 1899. [[CrossRef](#)]
130. Li, X.; Dong, G.; Liu, Z.; Zhang, X. Polyimide Aerogel Fibers with Superior Flame Resistance, Strength, Hydrophobicity, and Flexibility Made via a Universal Sol–Gel Confined Transition Strategy. *ACS Nano* **2021**, *15*, 4759–4768. [[CrossRef](#)]
131. Meng, S.; Zhang, J.; Chen, W.; Wang, X.; Zhu, M. Construction of continuous hollow silica aerogel fibers with hierarchical pores and excellent adsorption performance. *Microporous Mesoporous Mater.* **2019**, *273*, 294–296. [[CrossRef](#)]
132. Mitropoulos, A.N.; Burpo, F.J.; Nguyen, C.K.; Nagelli, E.A.; Ryu, M.Y.; Wang, J.; Sims, R.K.; Woronowicz, K.; Wickiser, J.K. Noble metal composite porous silk fibroin aerogel fibers. *Materials* **2019**, *12*, 894. [[CrossRef](#)]
133. Venkataraman, M.; Mishra, R.; Jasikova, D.; Kotresh, T.; Militky, J. Thermodynamics of aerogel-treated nonwoven fabrics at subzero temperatures. *J. Ind. Text.* **2015**, *45*, 387–404. [[CrossRef](#)]
134. Arshad, Z.; Alharthi, S.S. Enhancing the Thermal Comfort of Woven Fabrics and Mechanical Properties of Fiber-Reinforced Composites Using Multiple Weave Structures. *Fibers* **2023**, *11*, 73. [[CrossRef](#)]
135. Qian, H.; Kucernak, A.R.; Greenhalgh, E.S.; Bismarck, A.; Shaffer, M.S. Multifunctional structural supercapacitor composites based on carbon aerogel modified high performance carbon fiber fabric. *ACS Appl. Mater. Interfaces* **2013**, *5*, 6113–6122. [[CrossRef](#)]
136. Bhuiyan, M.R.; Wang, L.; Shaid, A.; Shanks, R.A.; Ding, J. Polyurethane-aerogel incorporated coating on cotton fabric for chemical protection. *Progr. Org. Coat.* **2019**, *131*, 100–110. [[CrossRef](#)]
137. Xiong, X.; Yang, T.; Mishra, R.; Militky, J. Transport properties of aerogel-based nanofibrous nonwoven fabrics. *Fibers Polym.* **2016**, *17*, 1709–1714. [[CrossRef](#)]
138. Talebi, Z.; Soltani, P.; Habibi, N.; Latifi, F. Silica aerogel/polyester blankets for efficient sound absorption in buildings. *Constr. Build. Mater.* **2019**, *220*, 76–89. [[CrossRef](#)]
139. Venkataraman, M.; Mishra, R.; Kotresh, T.; Sakoi, T.; Militky, J. Effect of compressibility on heat transport phenomena in aerogel-treated nonwoven fabrics. *J. Text. Inst.* **2016**, *107*, 1150–1158. [[CrossRef](#)]
140. Altay, P.; Atakan, R.; Özcan, G. Silica aerogel application to polyester fabric for outdoor clothing. *Fibers Polym.* **2021**, *22*, 1025–1032. [[CrossRef](#)]
141. Jabbari, M.; Åkesson, D.; Skrifvars, M.; Taherzadeh, M.J. Novel lightweight and highly thermally insulative silica aerogel-doped poly (vinyl chloride)-coated fabric composite. *J. Reinf. Plast. Compos.* **2015**, *34*, 1581–1592. [[CrossRef](#)]
142. Shaid, A.; Fergusson, M.; Wang, L. Thermophysiological comfort analysis of aerogel nanoparticle incorporated fabric for fire fighter’s protective clothing. *Chem. Mater. Eng.* **2014**, *2*, 37–43. [[CrossRef](#)]
143. Venkataraman, M.; Mishra, R.; Militky, J.; Hes, L. Aerogel based nanoporous fibrous materials for thermal insulation. *Fibers Polym.* **2014**, *15*, 1444–1449. [[CrossRef](#)]
144. Venkataraman, M.; Mishra, R.; Wiener, J.; Militky, J.; Kotresh, T.; Vaclavik, M. Novel techniques to analyse thermal performance of aerogel-treated blankets under extreme temperatures. *J. Text. Inst.* **2015**, *106*, 736–747. [[CrossRef](#)]
145. Han, Y.; Zhang, X.; Wu, X.; Lu, C. Flame retardant, heat insulating cellulose aerogels from waste cotton fabrics by in situ formation of magnesium hydroxide nanoparticles in cellulose gel nanostructures. *ACS Sustain. Chem. Eng.* **2015**, *3*, 1853–1859. [[CrossRef](#)]
146. Ahmad, F.; Ulker, Z.; Erkey, C. A novel composite of alginate aerogel with PET nonwoven with enhanced thermal resistance. *J. Non-Cryst. Solids* **2018**, *491*, 7–13. [[CrossRef](#)]
147. Lang, X.H.; Zhu, T.Y.; Zou, L.; Prakashan, K.; Zhang, Z.X. Fabrication and characterization of polypropylene aerogel material and aerogel coated hybrid materials for oil-water separation applications. *Prog. Org. Coat.* **2019**, *137*, 105370. [[CrossRef](#)]
148. Chakraborty, S.; Pisal, A.; Kothari, V.; Venkateswara Rao, A. Synthesis and characterization of fibre reinforced silica aerogel blankets for thermal protection. *Adv. Mater. Sci. Eng.* **2016**, *2016*, 2495623. [[CrossRef](#)]
149. Ibrahim, M.; Bianco, L.; Ibrahim, O.; Wurtz, E. Low-emissivity coating coupled with aerogel-based plaster for walls’ internal surface application in buildings: Energy saving potential based on thermal comfort assessment. *J. Build. Eng.* **2018**, *18*, 454–466. [[CrossRef](#)]

150. Masera, G.; Wakili, K.G.; Stahl, T.; Brunner, S.; Galliano, R.; Monticelli, C.; Aliprandi, S.; Zanelli, A.; Elesawy, A. Development of a super-insulating, aerogel-based textile wallpaper for the indoor energy retrofit of existing residential buildings. *Procedia Eng.* **2017**, *180*, 1139–1149. [[CrossRef](#)]
151. Schuss, M.; Pont, U.; Mahdavi, A. Long-term experimental performance evaluation of aerogel insulation plaster. *Energy Procedia* **2017**, *132*, 508–513. [[CrossRef](#)]
152. Wakili, K.G.; Stahl, T.; Heiduk, E.; Schuss, M.; Vonbank, R.; Pont, U.; Sustr, C.; Wolosiuk, D.; Mahdavi, A. High performance aerogel containing plaster for historic buildings with structured façades. *Energy Procedia* **2015**, *78*, 949–954. [[CrossRef](#)]
153. Schmidt, M.; Schwertfeger, F. Applications for silica aerogel products. *J. Non-Cryst. Solids* **1998**, *225*, 364–368. [[CrossRef](#)]
154. Fesmire, J.E. Aerogel insulation systems for space launch applications. *Cryogenics* **2006**, *46*, 111–117. [[CrossRef](#)]
155. Smirnova, I.; Gurikov, P. Aerogel production: Current status, research directions, and future opportunities. *J. Supercrit. Fluids* **2018**, *134*, 228–233. [[CrossRef](#)]
156. Pekala, R.; Farmer, J.; Alviso, C.; Tran, T.; Mayer, S.; Miller, J.; Dunn, B. Carbon aerogels for electrochemical applications. *J. Non-Cryst. Solids* **1998**, *225*, 74–80. [[CrossRef](#)]
157. Jelle, B.P.; Baetens, R.; Gustavsen, A. Aerogel insulation for building applications. In *The Sol-Gel Handbook*; Levy, D., Zayat, M., Eds.; Wiley-VCH: Weinheim, Germany, 2015; pp. 1385–1412.
158. Pierre, A.C.; Pajonk, G.M. Chemistry of aerogels and their applications. *Chem. Rev.* **2002**, *102*, 4243–4266. [[CrossRef](#)] [[PubMed](#)]
159. Zheng, L.; Zhang, S.; Ying, Z.; Liu, J.; Zhou, Y.; Chen, F. Engineering of aerogel-based biomaterials for biomedical applications. *Int. J. Nanomed.* **2020**, *15*, 2363. [[CrossRef](#)] [[PubMed](#)]
160. Long, L.-Y.; Weng, Y.-X.; Wang, Y.-Z. Cellulose aerogels: Synthesis, applications, and prospects. *Polymers* **2018**, *10*, 623. [[CrossRef](#)]
161. Fricke, J. Aerogels and their applications. *J. Non-Cryst. Solids* **1992**, *147*, 356–362. [[CrossRef](#)]
162. Linhares, T.; de Amorim, M.T.P.; Durães, L. Silica aerogel composites with embedded fibres: A review on their preparation, properties and applications. *J. Mater. Chem. A* **2019**, *7*, 22768–22802. [[CrossRef](#)]
163. Maleki, H. Recent advances in aerogels for environmental remediation applications: A review. *Chem. Eng. J.* **2016**, *300*, 98–118. [[CrossRef](#)]
164. Buratti, C.; Merli, F.; Moretti, E. Aerogel-based materials for building applications: Influence of granule size on thermal and acoustic performance. *Energy Build.* **2017**, *152*, 472–482. [[CrossRef](#)]
165. Moreno-Castilla, C.; Maldonado-Hódar, F. Carbon aerogels for catalysis applications: An overview. *Carbon* **2005**, *43*, 455–465. [[CrossRef](#)]
166. Fricke, J.; Emmerling, A. Aerogels—Recent progress in production techniques and novel applications. *J. Sol-Gel Sci. Technol.* **1998**, *13*, 299–303. [[CrossRef](#)]
167. Cuce, E.; Cuce, P.M.; Wood, C.J.; Riffat, S.B. Toward aerogel based thermal superinsulation in buildings: A comprehensive review. *Renew. Sustain. Energy Rev.* **2014**, *34*, 273–299. [[CrossRef](#)]
168. Hrubesh, L.W.; Poco, J.F. Thin aerogel films for optical, thermal, acoustic and electronic applications. *J. Non-Cryst. Solids* **1995**, *188*, 46–53. [[CrossRef](#)]
169. Zhao, S.; Malfait, W.J.; Guerrero-Alburquerque, N.; Koebel, M.M.; Nyström, G. Biopolymer aerogels and foams: Chemistry, properties, and applications. *Angew. Chem. Int. Ed.* **2018**, *57*, 7580–7608. [[CrossRef](#)]
170. Biener, J.; Stadermann, M.; Suss, M.; Worsley, M.A.; Biener, M.M.; Rose, K.A.; Baumann, T.F. Advanced carbon aerogels for energy applications. *Energy Environ. Sci.* **2011**, *4*, 656–667. [[CrossRef](#)]
171. Santos-Rosales, V.; Alvarez-Rivera, G.; Hillgärtner, M.; Cifuentes, A.; Itskov, M.; García-González, C.A.; Rege, A. Stability studies of starch aerogel formulations for biomedical applications. *Biomacromolecules* **2020**, *21*, 5336–5344. [[CrossRef](#)] [[PubMed](#)]
172. Li, F.; Xie, L.; Sun, G.; Kong, Q.; Su, F.; Cao, Y.; Wei, J.; Ahmad, A.; Guo, X.; Chen, C.-M. Resorcinol-formaldehyde based carbon aerogel: Preparation, structure and applications in energy storage devices. *Microporous Mesoporous Mater.* **2019**, *279*, 293–315. [[CrossRef](#)]
173. Hu, L.; He, R.; Lei, H.; Fang, D. Carbon aerogel for insulation applications: A review. *Int. J. Thermophys.* **2019**, *40*, 39. [[CrossRef](#)]
174. Stahl, T.; Brunner, S.; Zimmermann, M.; Wakili, K.G. Thermo-hygric properties of a newly developed aerogel based insulation rendering for both exterior and interior applications. *Energy Build.* **2012**, *44*, 114–117. [[CrossRef](#)]
175. Randall, J.P.; Meador, M.A.B.; Jana, S.C. Tailoring mechanical properties of aerogels for aerospace applications. *ACS Appl. Mater. Interfaces* **2011**, *3*, 613–626. [[CrossRef](#)]
176. López-Iglesias, C.; Barros, J.; Ardao, I.; Monteiro, F.J.; Alvarez-Lorenzo, C.; Gómez-Amoza, J.L.; García-González, C.A. Vancomycin-loaded chitosan aerogel particles for chronic wound applications. *Carbohydr. Polym.* **2019**, *204*, 223–231. [[CrossRef](#)]
177. Fricke, J.; Tillotson, T. Aerogels: Production, characterization, and applications. *Thin Solid Films* **1997**, *297*, 212–223. [[CrossRef](#)]
178. Cheng, Y.; Zhao, H.; Lv, H.; Shi, T.; Ji, G.; Hou, Y. Lightweight and flexible cotton aerogel composites for electromagnetic absorption and shielding applications. *Adv. Electron. Mater.* **2020**, *6*, 1900796. [[CrossRef](#)]
179. Olivito, F.; Algieri, V.; Jiritano, A.; Tallarida, M.A.; Costanzo, P.; Maiuolo, L.; De Nino, A. Bio-Based Polyurethane Foams for the Removal of Petroleum-Derived Pollutants: Sorption in Batch and in Continuous-Flow. *Polymers* **2023**, *15*, 1785. [[CrossRef](#)] [[PubMed](#)]
180. García-González, C.A.; Budtova, T.; Durães, L.; Erkey, C.; Del Gaudio, P.; Gurikov, P.; Koebel, M.; Liebner, F.; Neagu, M.; Smirnova, I. An opinion paper on aerogels for biomedical and environmental applications. *Molecules* **2019**, *24*, 1815. [[CrossRef](#)]

181. Ferreira-Neto, E.P.; Ullah, S.; Da Silva, T.C.; Domeneguetti, R.R.; Perissinotto, A.P.; De Vicente, F.S.; Rodrigues-Filho, U.P.; Ribeiro, S.J. Bacterial nanocellulose/MoS₂ hybrid aerogels as bifunctional adsorbent/photocatalyst membranes for in-flow water decontamination. *ACS Appl. Mater. Interfaces* **2020**, *12*, 41627–41643. [[CrossRef](#)] [[PubMed](#)]
182. Novak, Z.; Horvat, G. Book of Abstracts. In Proceedings of the 3rd International Conference on Aerogels for Biomedical and Environmental Applications, Maribor, Slovenia, 5–7 July 2023.
183. Lakatos, Á.; Trník, A. Thermal diffusion in fibrous aerogel blankets. *Energies* **2020**, *13*, 823. [[CrossRef](#)]

Disclaimer/Publisher's Note: The statements, opinions and data contained in all publications are solely those of the individual author(s) and contributor(s) and not of MDPI and/or the editor(s). MDPI and/or the editor(s) disclaim responsibility for any injury to people or property resulting from any ideas, methods, instructions or products referred to in the content.